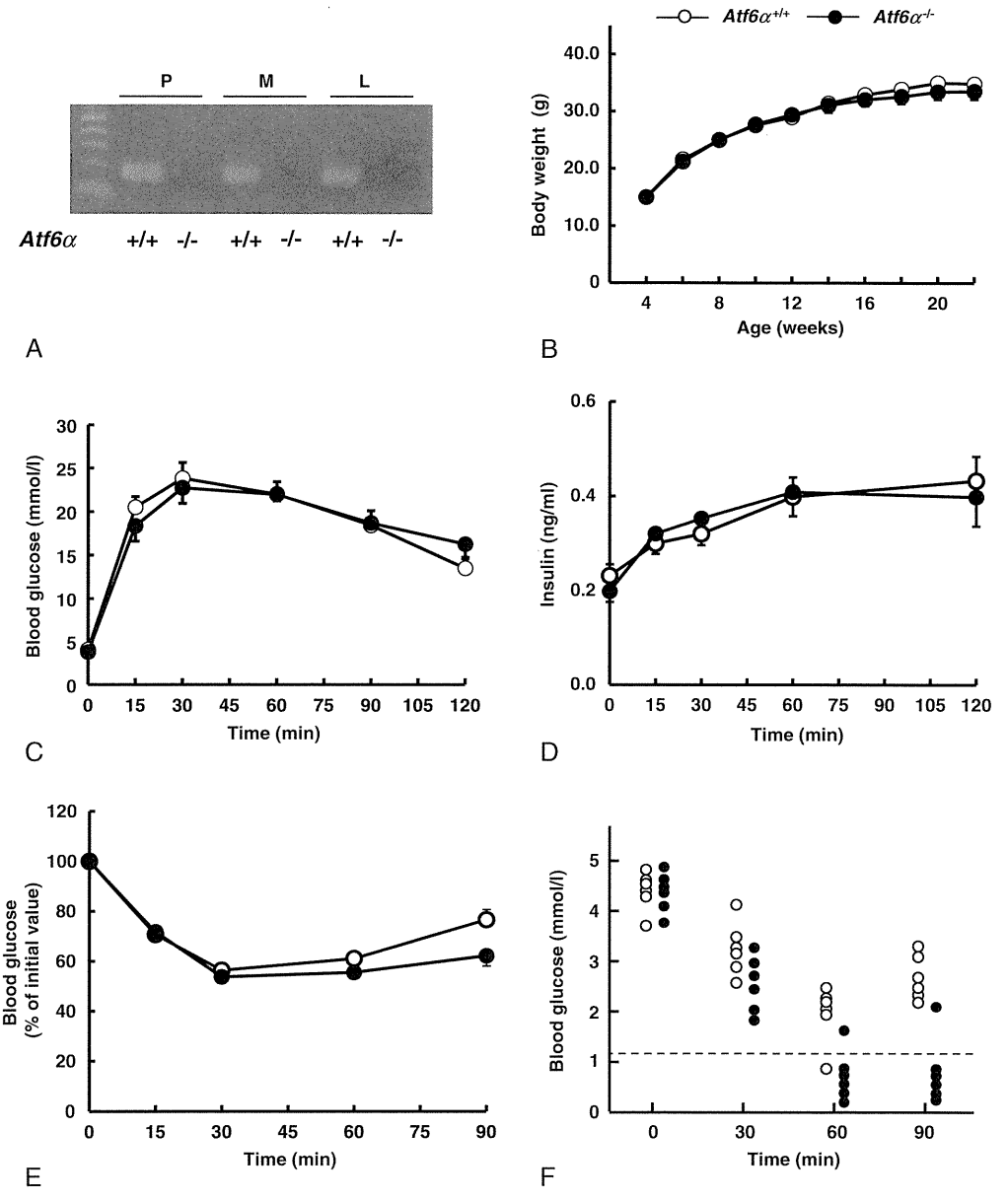

Fig. 1 – Glucose homeostasis in ATF6α-deficient mice fed with normal chow. A, Reverse transcription-PCR analysis of *Atf6α* mRNA expression in the pancreas (P), skeletal muscle (M) and liver (L) from *Atf6α*$^{+/+}$ and *Atf6α*$^{-/-}$ mice. B, Body weight of *Atf6α*$^{+/+}$ (white circles, *n* = 9) and *Atf6α*$^{-/-}$ (black circles, *n* = 13) mice. Data from three cohorts are combined. C and D, Intraperitoneal glucose tolerance tests (2 g/kg body weight) were performed at 17–19 weeks of age in *Atf6α*$^{+/+}$ (white circles, *n* = 9) and *Atf6α*$^{-/-}$ (black circles, *n* = 13) mice. Blood glucose (C) and plasma immunoreactive insulin levels (D) were measured. E, Insulin tolerance test (0.75 U/kg body weight) was performed at 21 weeks of age in *Atf6α*$^{+/+}$ (white circles, *n* = 7) and *Atf6α*$^{-/-}$ (black circles, *n* = 9) mice. F, Insulin tolerance test (2.0 U/kg body weight) was performed at 23 weeks of age in *Atf6α*$^{+/+}$ (white circles, *n* = 6) and *Atf6α*$^{-/-}$ (black circles, *n* = 6) mice. In one *Atf6α*$^{+/+}$ mouse at 60 min and 5 *Atf6α*$^{-/-}$ mice at 60 and 90 min, blood glucose levels were below the detection limit (1.1 mM, dashed line).

deficient DO mice tended to gain less weight (Fig. 2A) and showed similar blood glucose levels to those of WT-DO mice at non-fasted states (Fig. 2B). An IPGTT exhibited that ATF6α-deficient DO mice were less glucose tolerant (Fig. 2C) with reduced insulin secretion (Fig. 2D). On an HFD, it was evident that ATF6α-deficient mice were more insulin sensitive (Fig. 2E). We also measured serum lipid content in these mice. As shown in Fig. 2F, an HFD-induced increase in the serum triglyceride (TG) concentration was partially suppressed in *Atf6α*$^{-/-}$DO mice.

3.3. *Pancreatic β-cells suffered from ER stress in ATF6α-deficient mice fed with a high fat diet*

Although serum insulin levels in *Atf6α*$^{-/-}$DO mice (Fig. 2D) were lower than those in WT-DO mice, they were 3 times

Please cite this article as: Usui M, et al, Atf6α-null mice are glucose intolerant due to pancreatic β-cell failure on a high-fat diet but partially resistant to diet-induced..., Metabolism (2012), doi:10.1016/j.metabol.2012.01.004

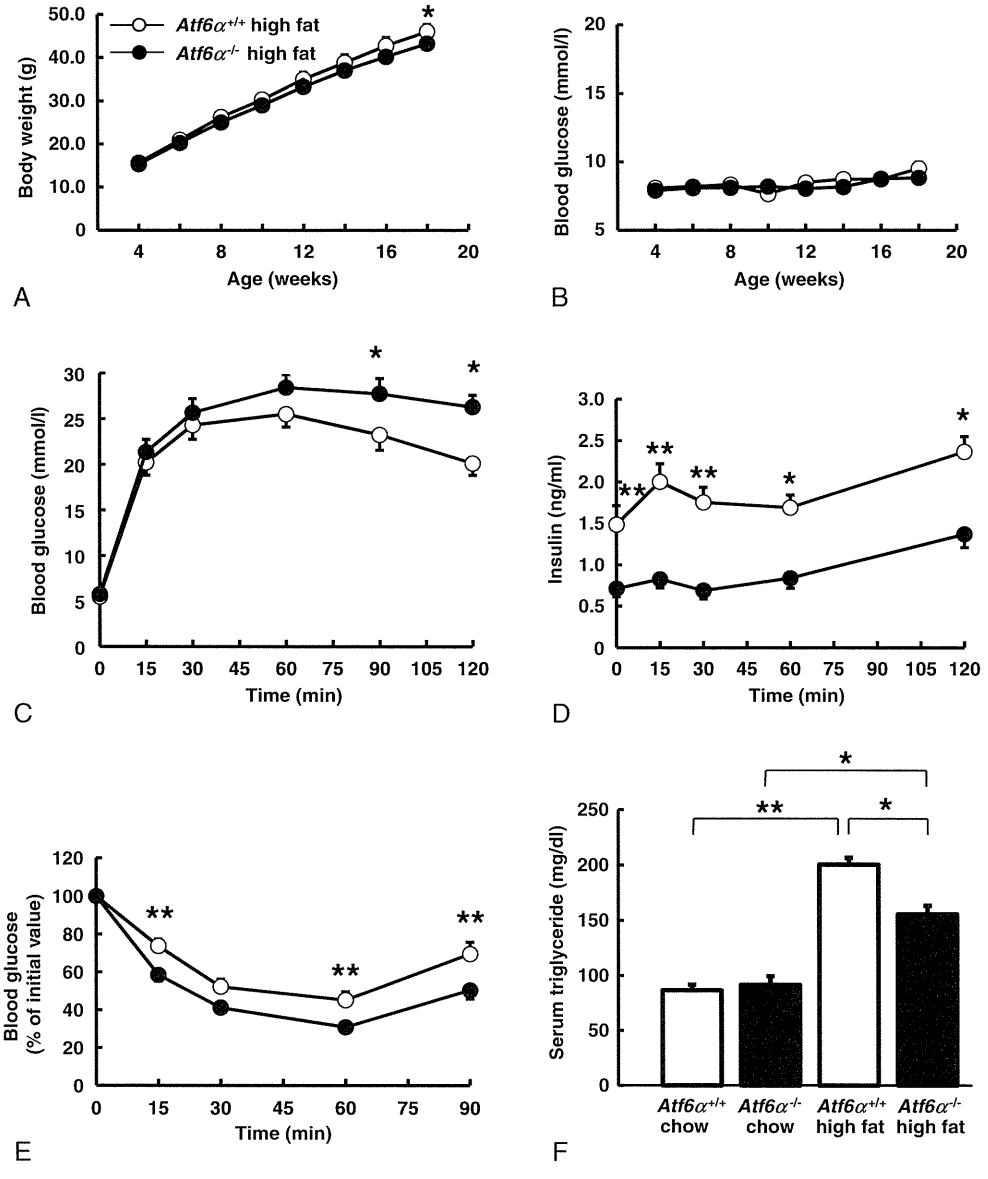

Fig. 2 – Metabolic homeostasis in ATF6α-deficient mice fed with an HFD. A and B, Body weight (A) and non-fasted glucose (B) were measured in *Atf6α*$^{+/+}$ (white circles, *n* = 12) and *Atf6α*$^{-/-}$ (black circles, *n* = 17) mice fed with an HFD. *P < .05. C and D, Intraperitoneal glucose tolerance test (1.5 g/kg body weight) was performed at 17–19 weeks of age in *Atf6α*$^{+/+}$ (white circles, *n* = 12) and *Atf6α*$^{-/-}$ (black circles, *n* = 17) mice on an HFD. Blood glucose (C) and plasma immunoreactive insulin levels (D) were measured. *P < .05, **P < .01. E, Insulin tolerance test (1.5 U/kg) was performed at 20–22 weeks of age in *Atf6α*$^{+/+}$ (white circles, *n* = 12) and *Atf6α*$^{-/-}$ (black circles, *n* = 17) mice on an HFD. **P < .01. F, Serum triglyceride levels were measured at the 17–19 weeks of age in *Atf6α*$^{+/+}$ (*n* = 8) and *Atf6α*$^{-/-}$ (*n* = 7) mice on normal chow as well as *Atf6α*$^{+/+}$ (*n* = 11) and *Atf6α*$^{-/-}$ (*n* = 13) mice on an HFD. *P < .05, **P < .01.

higher than those in ATF6α-deficient mice fed with normal chow (Fig. 1D). The homeostasis model assessment of insulin resistance index was 2.20, 1.66, 9.81 and 4.58, for WT on normal chow, *Atf6α*$^{-/-}$ on normal chow, WT on an HFD and *Atf6α*$^{-/-}$ on an HFD, respectively. These results indicated that *Atf6α*$^{-/-}$DO mice developed insulin resistance, although milder than WT mice. Therefore, it was reasonable to speculate that lower insulin secretion in *Atf6α*$^{-/-}$DO mice could result from β-cell failure in adaptation to increased insulin resistance. In order to gain insight into β-cell homeostasis in *Atf6α*$^{-/-}$DO mice, pancreatic insulin content was measured. While pancreatic insulin content increased upon HFD feeding in WT mice, *Atf6α*$^{-/-}$ mice did not respond to the HFD by increasing insulin production (Fig. 3A). We then analyzed ultrastructure of β-cells in *Atf6α*$^{-/-}$ mice fed with an HFD. As indicated in Fig. 3B, while the ER in β-cells showed compact reticulate structure in WT-DO mice, in *Atf6α*$^{-/-}$DO mouse β-cells, frequently observed was swollen ER, a typical phenotype of ER stressed cells [29]. These data indicate that ATF6α-deficient β-cells suffered from ER stress due to increased demands of insulin production, and suggest that lower insulin secretion was, at least partly, caused by ER

Please cite this article as: Usui M, et al, Atf6α-null mice are glucose intolerant due to pancreatic β-cell failure on a high-fat diet but partially resistant to diet-induced..., Metabolism (2012), doi:10.1016/j.metabol.2012.01.004

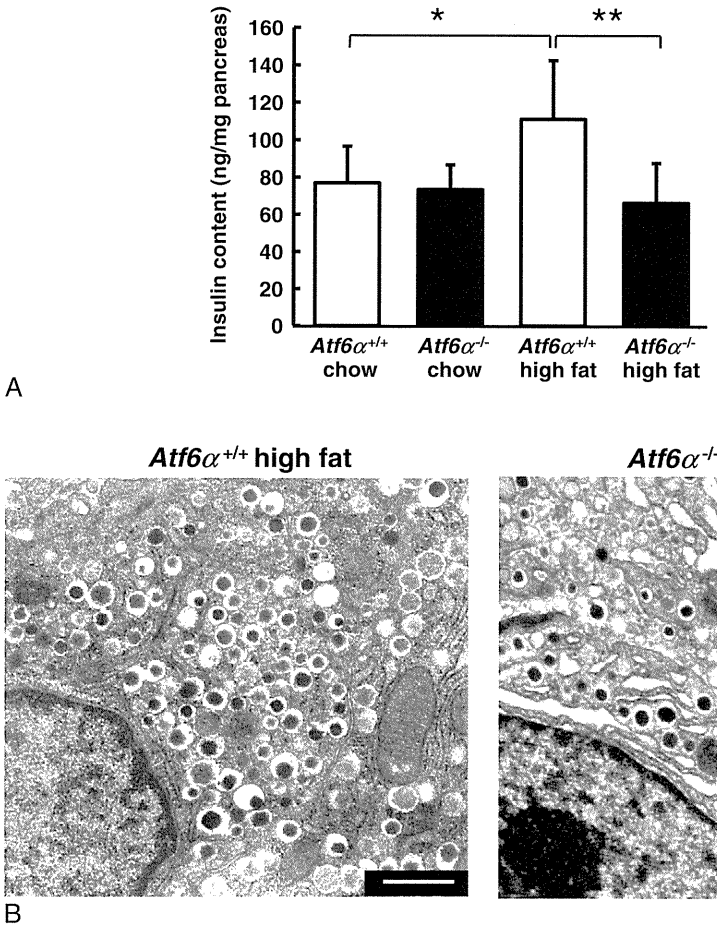

Fig. 3 – Pancreatic β-cell homeostasis in *Atf6α*$^{-/-}$ mice on an HFD. A, Pancreatic insulin content was measured in *Atf6α*$^{+/+}$ (n = 6) and *Atf6α*$^{-/-}$ (n = 5) mice on normal chow as well as *Atf6α*$^{+/+}$ (n = 10) and *Atf6α*$^{-/-}$ (n = 13) mice on an HFD at 25 weeks of age. *P < .05, **P < .01. B, Ultrastructural analysis was performed on islets of *Atf6α*$^{+/+}$ (n = 3) and *Atf6α*$^{-/-}$ (n = 3) mice on HFD at 25 weeks of age. Representative micrographs of β-cells are shown. Bars, 1 μm.

stress-induced failure in maintaining insulin content in ATF6α-deficient pancreas.

3.4. *Impact of ATF6 deficiency on liver homeostasis in mice fed with a high fat diet*

It is known that ER stress is increased in the liver of HFD-fed mice [7]. Thus, we analyzed effects of ATF6α deficiency on UPR gene expressions in the liver. XBP-1 mRNA splicing was augmented (Fig. 4A) and ATF4 mRNA levels was increased (Fig. 4B) in livers of *Atf6α*$^{-/-}$DO mice, indicating that higher ER stress existed when the ATF6α-deficient liver was metabolically overloaded. Since recent studies have indicated the involvement of UPR mediators in hepatic lipogenesis or glycolysis [30,31], we measured expressions of lipogenic or glycolytic enzymes. We found that mRNA expressions of a gluconeogenic enzyme glucose-6-phosphatase (G6P) and those of PPAR-γ and SREBP1c, master regulators of lipogenic enzymes, were increased in ATF6α-deficient DO mice (Fig. 4B). These findings have prompted us to measure liver TG content and to conduct morphological analysis of the liver in these animals. Liver TG content tended to increase in *Atf6α*$^{-/-}$DO mice although the difference failed to reach statistical significance (P = .069, Fig. 4C). Liver sections showed increased lipid droplets in *Atf6α*$^{-/-}$DO mice (Fig. 4D), suggesting that steatosis was enhanced with ATF6α deficiency.

3.5. *ATF6α deficiency in Agouti yellow obese mice, a genetic diabetes model with increased insulin resistance*

To confirm effects of ATF6α deficiency on insulin resistance, ATF6α-deficient mice were crossed with Agouti yellow (A^y) mice. A^y mice develop obesity and insulin resistance because of blockade of hypothalamic melanocortin-4 receptors due to ectopic expression of agouti peptide and thus are resistant to the satiety [32,33]. The phenotypes of *Atf6α*$^{-/-}$$A^y$ mice were similar to those of *Atf6α*$^{-/-}$DO mice. Body weights of *Atf6α*$^{-/-}$$A^y$ mice were significantly lower than those of A^y mice (Fig. 5A). Although blood glucose levels were similar between the two strains (Fig. 5B), glucose excursion after an intraperitoneal glucose challenge was greater with reduced insulin secretion in *Atf6α*$^{-/-}$$A^y$ mice (Figs. 5C and 5D). Insulin sensitivity estimated by ITT was also higher in ATF6α-deficient A^y mice (Fig. 5E). Pancreatic insulin content was approximately 50% lower in *Atf6α*$^{-/-}$$A^y$ mice than in WT mice at 25 weeks of age (Fig. 5F).

Please cite this article as: Usui M, et al, Atf6α-null mice are glucose intolerant due to pancreatic β-cell failure on a high-fat diet but partially resistant to diet-induced..., Metabolism (2012), doi:10.1016/j.metabol.2012.01.004

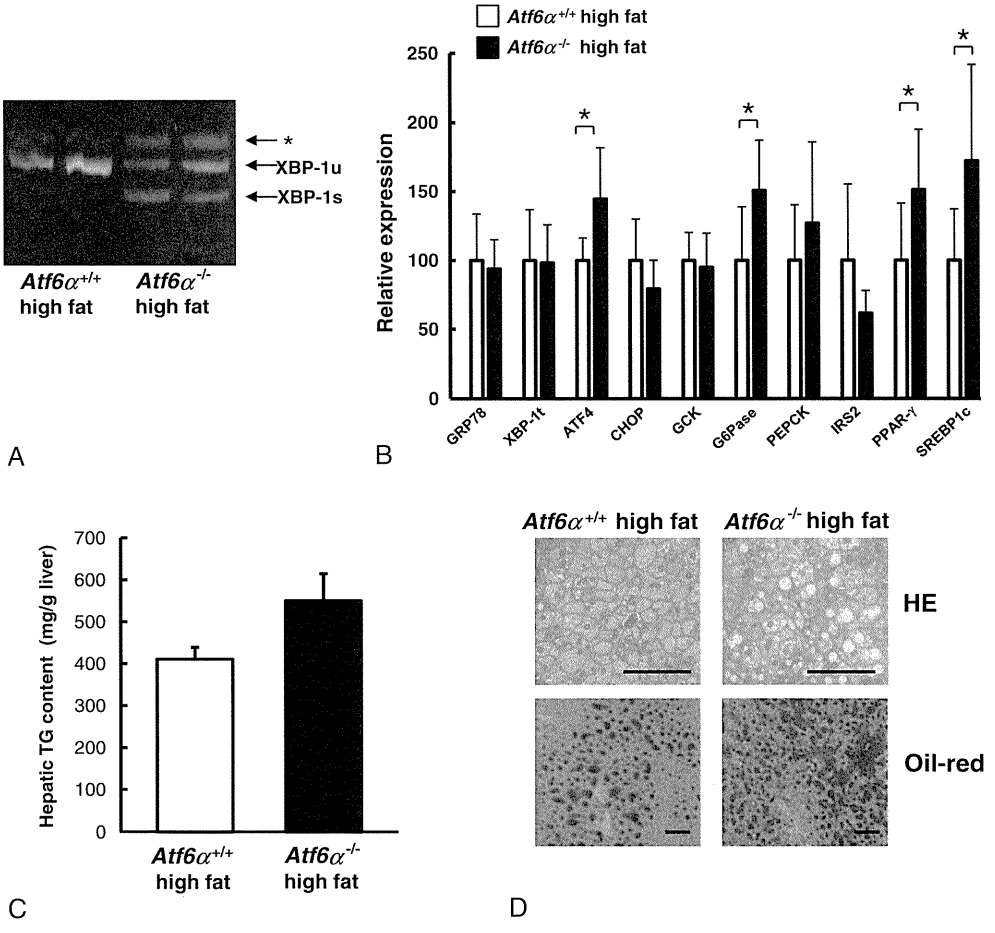

Fig. 4 – Impact of ATF6 deficiency on liver homeostasis in mice on an HFD. A, Spliced (XBP-1s) and unspliced (XBP-1u) forms of XBP-1 mRNA were analyzed in liver of WT and *Atf6α*$^{-/-}$ mice on an HFD. The data are representative of 5 experiments. *Non-specific band. B, Quantitative RT-PCR was conducted using total RNA extracted from *Atf6α*$^{+/+}$ (n = 6) and *Atf6α*$^{-/-}$ (n = 11) mouse liver on an HFD at 25 weeks of age. XBP-1t: total XBP-1 mRNA. Data are presented as β-actin corrected value ± SD. *$P < .05$. C, TG content of liver was measured using liver homogenates from *Atf6α*$^{+/+}$ (white bars, n = 7) and *Atf6α*$^{-/-}$ (black bars, n = 9) mice on an HFD at 21 weeks of age. D, *Atf6α*$^{+/+}$ and *Atf6α*$^{-/-}$ mouse liver sections were stained with hematoxylin–eosin and oil-red O at 25 weeks of age. Bars, 100 μm.

3.6. *ATF6α deficiency in* $Ins2^{WT/C96Y}$ *mice, a genetic diabetes model with ER-stress induced β-cell failure*

Studies on pancreas of *Atf6α*$^{-/-}$DO mice showed that ATF6-deficient β-cells suffered from ER stress. Thus, roles of ATF6α in β-cells under ER stress were also studied in *Atf6α*$^{-/-}$ mice bred with $Ins2^{WT/C96Y}$ (Akita) mice. In the latter mutant mice, insulin molecule with a Cys96Tyr mutation cannot fold correctly and causes ER stress in β-cells, leading to β-cell death and diabetes [27]. Reduction in BW and exaggerated hyperglycemia were evident in *Atf6α*$^{-/-}$$Ins2^{WT/C96Y}$ mice compared with *Atf6α*$^{+/+}$$Ins2^{WT/C96Y}$ mice (Figs. 6A and 6B). Pancreas insulin content from *Atf6α*$^{-/-}$$Ins2^{WT/C96Y}$ mice was 50% of that from *Atf6α*$^{+/+}$ $Ins2^{WT/C96Y}$ mice at 4–5 weeks of age, which was already reduced to one-third that from WT pancreas (Fig. 6C), with the majority of islets being smaller than those in $Ins2^{WT/C96Y}$ mice (Fig. 6D). These data showed that ATF6α contributes to the protection of β-cells against ER stress caused by mutated insulin Cys96Tyr in vivo.

4. Discussion

ATF6α, an ER stress sensor molecule, plays a critical role in initiation and development of the UPR. Recent studies indicated that ER stress itself and/or the UPR signaling are implicated in several components of the diabetes pathophysiology, including reduced β-cell mass, increased insulin resistance, ectopic lipid accumulation and hyperlipidemia. Thus, it has been speculated that ATF6α deficiency would have an impact on metabolic homeostasis. Our analysis of ATF6α-deficient mice revealed that ATF6α contributes to both prevention and promotion of the metabolic disorder in vivo.

In the absence of environmental challenges, *Atf6α*$^{-/-}$ mice maintained normal glucose homeostasis with normal insulin secretory responses, indicating that β-cells without ATF6α have the capacity to deal with the large amount of proinsulin under the physiological condition. However, when metabolic overload further demanded to produce and secrete greater

Please cite this article as: Usui M, et al, Atf6α-null mice are glucose intolerant due to pancreatic β-cell failure on a high-fat diet but partially resistant to diet-induced..., Metabolism (2012), doi:10.1016/j.metabol.2012.01.004

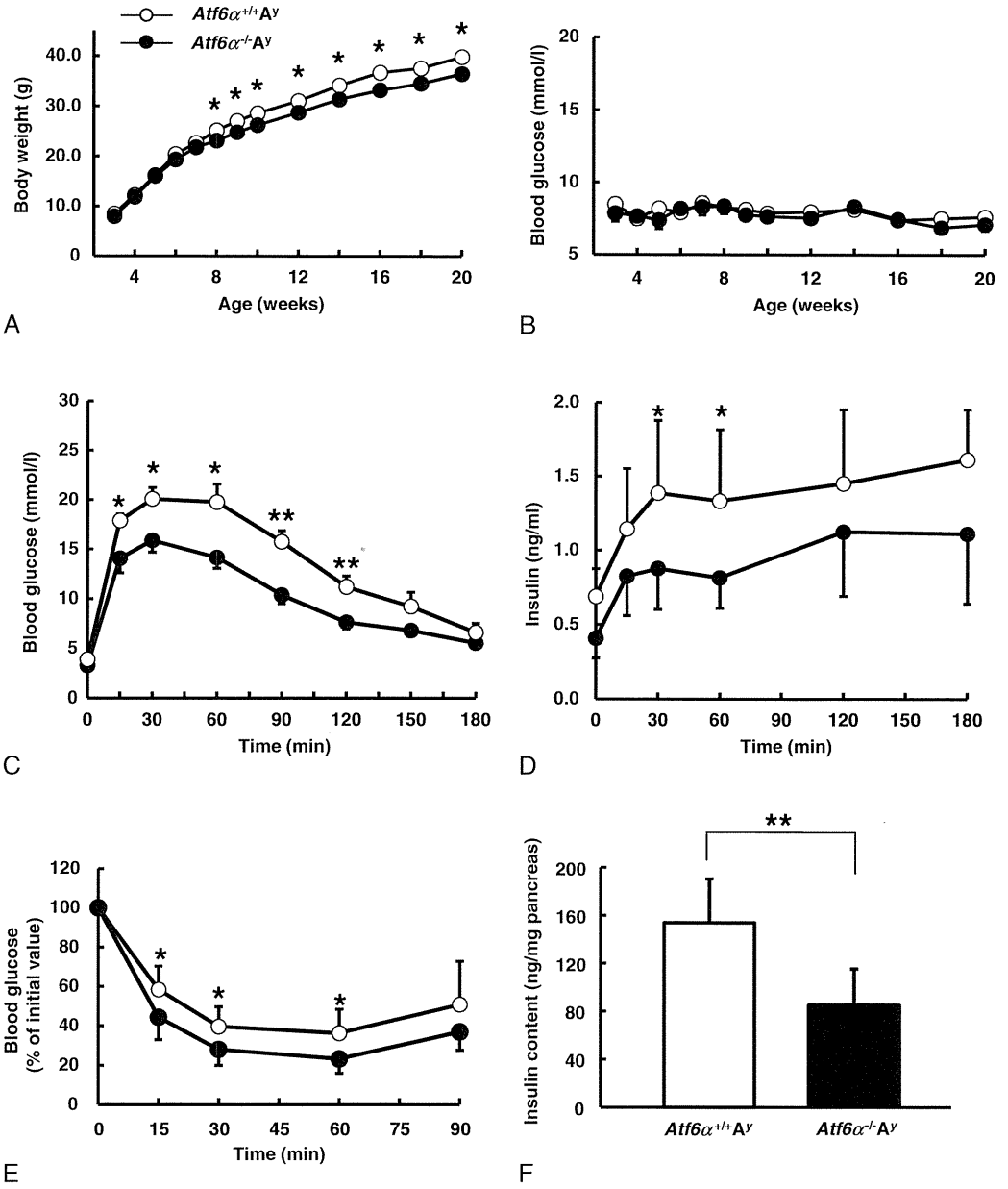

Fig. 5 – Glucose homeostasis in ATF6α-deficient A^y mice. A and B, Body weight (A) and glucose levels (B) on fed conditions were measured in $Atf6\alpha^{+/+}A^y$ (white circles, $n = 10$) and $Atf6\alpha^{-/-}A^y$ (black circles, $n = 13$) mice. Data from four cohorts are combined. *P < .05. C and D, Intraperitoneal glucose tolerance tests (1.5 g/kg body weight) were performed at 17–19 weeks of age in $Atf6\alpha^{+/+}A^y$ (white circles, $n = 7$) and $Atf6\alpha^{-/-}A^y$ (black circles, $n = 8$) mice. Blood glucose (C) and plasma immunoreactive insulin levels (D) were measured. *P < .05, **P < .01. E, Insulin tolerance tests (1.5 U/kg) were performed (E) at 20–22 weeks of age in $Atf6\alpha^{+/+}A^y$ (white circles, $n = 7$) and $Atf6\alpha^{-/-}A^y$ (black circles, $n = 8$) mice. *P < .05. F: Pancreatic insulin content was measured in $Atf6\alpha^{+/+}A^y$ ($n = 6$) and $Atf6\alpha^{-/-}A^y$ ($n = 8$) mice at 25 weeks of age. **P < .01.

amount of insulin, the ATF6α-deficient β-cell failed to cope with the stress. Thus, we observed swollen ER, a typical phenotype of the stressed ER [29], in the β-cell of $Atf6\alpha^{-/-}$DO mice. The β-cell failure under the HFD seemed to be also caused by increased circulating lipid levels, as lipotoxicity is also a cause of ER stress [34]. We did not examine β-cell mass in $Atf6\alpha^{-/-}$DO mice. Therefore, it was not clear that lower pancreatic insulin content in $Atf6\alpha^{-/-}$DO mice resulted either from reduced insulin production in individual β-cells or from reduction in β-cell mass. Nonetheless, we prefer the latter possibility, since islets became smaller when the *Atf6α* gene was deleted in β-cells with misfolded insulin molecules in Akita $Ins2^{WT/C96Y}$ mice. These data suggest that ATF6α plays an important role in β-cell survival under ER stress conditions.

It has been known that ER stress plays a role in metabolic regulation in the liver. ATF6α reportedly suppresses gluconeogenesis by inhibiting transcription of gluconeogenic enzymes [35,36]. In accordance with this notion, we observed increased G6P expression, possibly contributing to impaired glucose homeostasis in ATF6α-deficient DO mice.

Please cite this article as: Usui M, et al, Atf6α-null mice are glucose intolerant due to pancreatic β-cell failure on a high-fat diet but partially resistant to diet-induced..., Metabolism (2012), doi:10.1016/j.metabol.2012.01.004

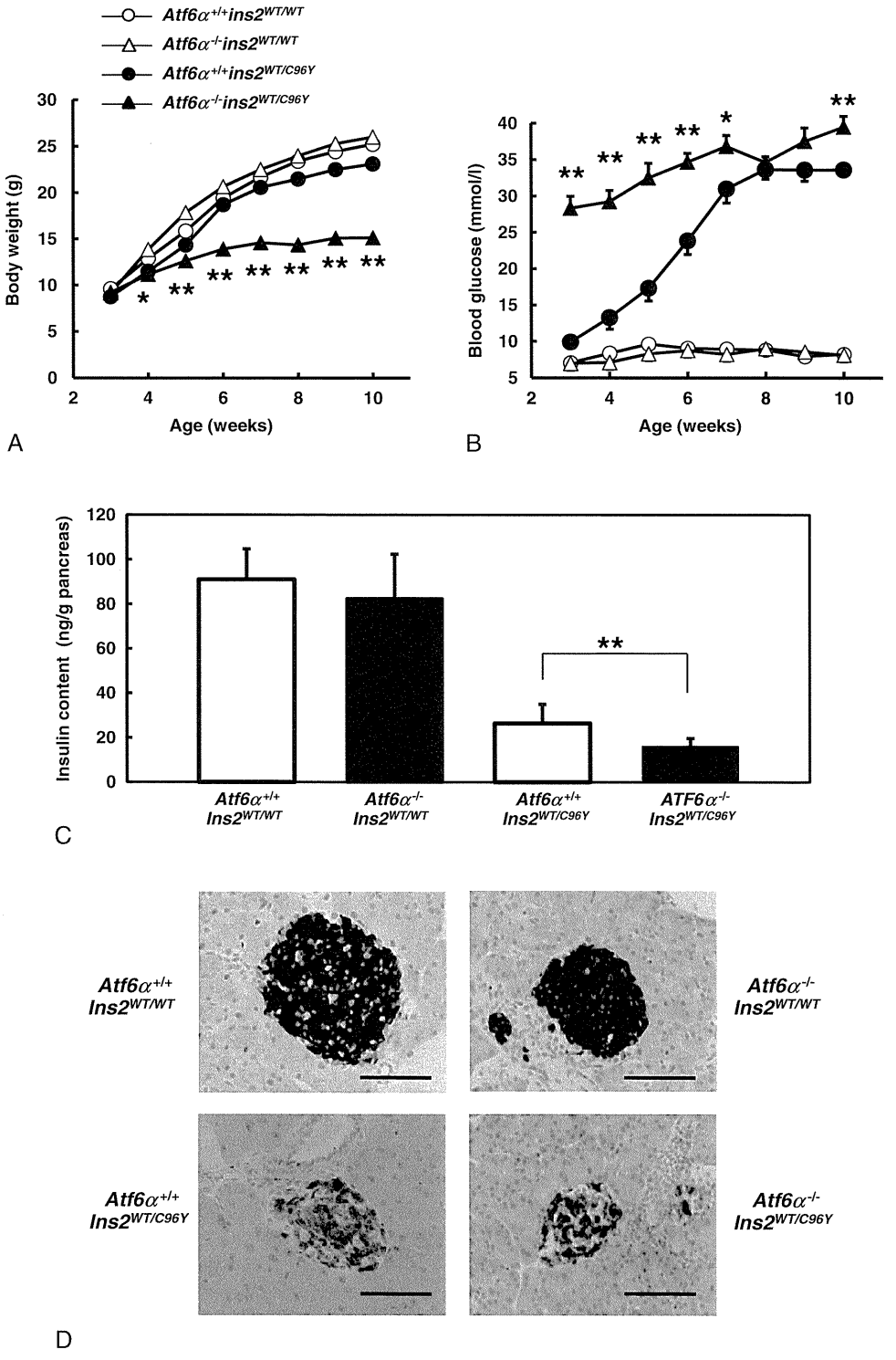

Fig. 6 – ATF6α deficiency exaggerated hyperglycemia in $Ins2^{WT/C96Y}$ mice. A and B, Body weight (A) and glucose levels (B) on fed conditions were measured in $Atf6\alpha^{+/+}$ (white circles, n = 12), $Atf6\alpha^{+/+}Ins2^{WT/C96Y}$ (black circles, n = 16), $Atf6\alpha^{-/-}$ (white triangles, n = 13) and $Atf6\alpha^{-/-}Ins2^{WT/C96Y}$ (black triangles, n = 15) mice. *P < .05, **P < .01 compared with the $Atf6\alpha^{+/+}Ins2^{WT/C96Y}$ mice. C, Pancreatic insulin content of $Atf6\alpha^{+/+}$ (n = 8), $Atf6\alpha^{-/-}$(n = 9), $Atf6\alpha^{+/+}Ins2^{WT/C96Y}$ (n = 11) and $Atf6\alpha^{-/-}Ins2^{WT/C96Y}$ (n = 11) mice at 4–5 weeks of age. **P < .01. D, Pancreas section of mice with indicated genotypes at 4–5 weeks of age was immunostained for insulin. Bars, 100 μm.

Recent studies have also revealed a link between ER stress and hepatic steatosis. $Atf6\alpha^{-/-}$ mice [19,37], mice with liver-specific deletion of functional eIF2α [19], and liver-specific IRE1α knockout mice [19], all developed hepatic steatosis when a pharmacological ER stress inducer, tunicamycin (a protein glycosylation inhibitor) was injected. Here, we

Please cite this article as: Usui M, et al, Atf6α-null mice are glucose intolerant due to pancreatic β-cell failure on a high-fat diet but partially resistant to diet-induced..., Metabolism (2012), doi:10.1016/j.metabol.2012.01.004

demonstrated that greater levels of ER stress were present with increased tendency to develop a higher degree of hepatosteatosis in liver of ATF6α-deficient DO mice. Thus, our data indicate that not only acute pharmacological ER stress but also chronic ER stress promoted the development of hepatosteatosis. It has been postulated that ER stress-mediated activation of metabolic master regulator proteins, such as PPAR-γ and SREBP1c, contributes to liver steatosis [19,30]. A direct role of ATF6α in regulation of lipid homeostasis has been also postulated: ATF6α attenuates lipogenesis in the liver by suppressing SERBP2 [38]. Interestingly, we observed that despite increased lipid accumulation in the liver, circulating triglyceride levels were lower in *Atf6α*$^{-/-}$DO mice. These data suggest defects in impaired very low-density lipoprotein (VLDL) formation or triglyceride transfer to the circulation. A recent article indicated that ER stress-mediated reduction in stability of apolipoprotein B-100, a major protein component of VLDL, caused lipid accumulation in the liver of *Atf6α*$^{-/-}$ mice injected with tunicamycin [37]. A similar mechanism might be involved in the liver of *Atf6α*$^{-/-}$DO mice under chronic ER stress, which leads to liver steatosis.

An interesting observation made in this study was that ATF6α deficiency resulted in improved insulin sensitivity. *Atf6α*-null mice were partially resistant to development of insulin resistance resulting from metabolic overload induced by two different manners: placing on a high fat diet or introducing the agouti mutation causing hyperphagia. The mechanism by which ATF6α deficiency made mice partially resistant to the development of insulin resistance is currently unknown. It has been shown that the serum triglyceride level is a factor of insulin resistance [39,40]. Therefore, partial suppression in the development of hypertriglyceridemia might cause improved insulin sensitivity in ATF6α-deficient DO mice.

The present data indicate that ATF6α protects pancreatic β-cells from ER stress-induced cell damage. It also seems to protect liver tissue from steatosis under the HFD, but contributes to development of hyperlipidemia and insulin resistance in mice. Thus, ATF6α affects whole body glucose homeostasis through tissue specific actions. A limitation of the present study, in which whole body knockout mice were analyzed, is that some phenotypes of one tissue could be influenced by those of other tissues with ATF6α deficiency. Future studies using tissue specific ATF6α knockout mice would clarify these issues.

Supplementary materials related to this article can be found online at doi:10.1016/j.metabol.2012.01.004.

Funding

This research was supported by a Grant-in-Aid for Scientific Research (H16-genome-003) to Y.O. from the Ministry of Health, Labor and Welfare of Japan. This work was also supported by the 21st Global COE Program to Y.O. and a Grant-in-Aid for Scientific Research (21591147) to H.I. from the Ministry of Education, Science, Sports and Culture of Japan and a research grant from the Takeda Science Foundation to H.I.

Acknowledgment

We are grateful to C. Suzuki and M. Kato for their expert technical assistance.

REFERENCES

[1] Kasuga M. Insulin resistance and pancreatic β cell failure. J Clin Invest 2006;116:1756-60.
[2] Sakuraba H, Mizukami H, Yagihashi N, et al. Reduced β-cell mass and expression of oxidative stress-related DNA damage in the islet of Japanese type II diabetic patients. Diabetologia 2002;45:85-96.
[3] Butler AE, Janson J, Soeller WC, et al. Increased β-cell apoptosis prevents adaptive increase in β-cell mass in mouse model of type 2 diabetes: evidence for role of islet amyloid formation rather than direct action of amyloid. Diabetes 2003;52:2304-14.
[4] Rahier J, Guiot Y, Goebbels RM, et al. Pancreatic β-cell mass in European subjects with type 2 diabetes. Diabetes Obes Metab 2008;10(Suppl 4):32-42.
[5] Eizirik DL, Cardozo AK, Cnop M. The role for endoplasmic reticulum stress in diabetes mellitus. Endocr Rev 2008;29: 42-61.
[6] Scheuner D, Kaufman RJ. The unfolded protein response: a pathway that links insulin demand with β-cell failure and diabetes. Endocr Rev 2008;29:317-33.
[7] Ozcan U, Cao Q, Yilmaz E, et al. Endoplasmic reticulum stress links obesity, insulin action, and type 2 diabetes. Science 2004;306:457-61.
[8] Hotamisligil GS. Endoplasmic reticulumn stress and the inflamatory basis of metabolic disease. Cell 2010;140:900-17.
[9] Boden G, Duan X, Homko C, et al. Increase in endoplasmic reticulum stress-related proteins and genes in adipose tissue of obese, insulin-resistant individuals. Diabetes 2008;57: 2438-44.
[10] Gregor MF, Yang L, Fabbrini E, et al. Endoplasmic reticulum stress is reduced in tissues of obese subjects after weight loss. Diabetes 2009;58:693-700.
[11] Sharma NK, Das SK, Mondal AK, et al. Endoplasmic reticulum stress markers are associated with obesity in nondiabetic subjects. J Clin Endocrinol Metab 2008;93:4532-41.
[12] Ron D, Walter P. Signal integration in the endoplasmic reticulum unfolded protein response. Nat Rev Mol Cell Biol 2007;8:519-29.
[13] Oslowski CM, Urano F. A switch from life to death in endoplasmic reticulum stressed β-cells. Diabetes Obes Metab 2010;12(Suppl 2):58-65.
[14] Harding HP, Zhang Y, Ron D. Protein translation and folding are coupled by an endoplasmic-reticulum-resident kinase. Nature 1999;397:271-4.
[15] Harding HP, Zeng H, Zhang Y, et al. Diabetes mellitus and exocrine pancreatic dysfunction in perk–/– mice reveals a role for translational control in secretory cell survival. Mol Cell 2001;7:1153-63.
[16] Urano F, Wang X, Bertolotti A, et al. Coupling of stress in the ER to activation of JNK protein kinases by transmembrane protein kinase IRE1. Science 2000;287:664-6.
[17] Delepine M, Nicolino M, Barrett T, et al. EIF2AK3, encoding translation initiation factor 2-α kinase 3, is mutated in patients with Wolcott-Rallison syndrome. Nat Genet 2000;25: 406-9.
[18] Rutkowski DT, Wu J, Back SH, et al. UPR pathways combine to prevent hepatic steatosis caused by ER stress-mediated suppression of transcriptional master regulators. Dev Cell 2008;15:829-40.

Please cite this article as: Usui M, et al, Atf6α-null mice are glucose intolerant due to pancreatic β-cell failure on a high-fat diet but partially resistant to diet-induced..., Metabolism (2012), doi:10.1016/j.metabol.2012.01.004

[19] Wu J, Rutkowski DT, Dubois M, et al. ATF6α optimizes long-term endoplasmic reticulum function to protect cells from chronic stress. Dev Cell 2007;13:351-64.
[20] Yamamoto K, Sato T, Matsui T, et al. Transcriptional induction of mammalian ER quality control proteins is mediated by single or combined action of ATF6α and XBP1. Dev Cell 2007;13:365-76.
[21] Laybutt DR, Preston AM, Akerfeldt MC, et al. Endoplasmic reticulum stress contributes to β cell apoptosis in type 2 diabetes. Diabetologia 2007;50:752-63.
[22] Meex SJ, Weissglas-Volkov D, van der Kallen CJ, et al. The ATF6-Met[67]Val substitution is associated with increased plasma cholesterol levels. Arterioscler Thromb Vasc Biol 2009;29:1322-7.
[23] Chu WS, Das SK, Wang H, et al. Activating transcription factor 6 (ATF6) sequence polymorphisms in type 2 diabetes and pre-diabetic traits. Diabetes 2007;56:856-62.
[24] Meex SJ, van Greevenbroek MM, Ayoubi TA, et al. Activating transcription factor 6 polymorphisms and haplotypes are associated with impaired glucose homeostasis and type 2 diabetes in Dutch Caucasians. J Clin Endocrinol Metab 2007;92:2720-5.
[25] Thameem F, Farook VS, Bogardus C, et al. Association of amino acid variants in the activating transcription factor 6 gene (ATF6) on 1q21-q23 with type 2 diabetes in Pima Indians. Diabetes 2006;55:839-42.
[26] Hu C, Zhang R, Wang C, et al. Lack of association between genetic polymorphisms within DUSP12 - ATF6 locus and glucose metabolism related traits in a Chinese population. BMC Med Genet 2011;12:3.
[27] Wang J, Takeuchi T, Tanaka S, et al. A mutation in the insulin 2 gene induces diabetes with severe pancreatic β-cell dysfunction in the Mody mouse. J Clin Invest 1999;103:27-37.
[28] Folch J, Lees M, Sloane Stanley GH. A simple method for the isolation and purification of total lipides from animal tissues. J Biol Chem 1957;226:497-509.
[29] Scheuner D, van der Mierde D, Song B, et al. Control of mRNA translation preserves endoplasmic reticulum function in β cells and maintains glucose homeostasis. Nat Med 2005;11: 757-64.
[30] Kammoun HL, Chabanon H, Hainault I, et al. GRP78 expression inhibits insulin and ER stress-induced SREBP-1c activation and reduces hepatic steatosis in mice. J Clin Invest 2009;119:1201-15.
[31] Liu J, Jin X, Yu CH, et al. Endoplasmic reticulum stress involved in the course of lipogenesis in fatty acids-induced hepatic steatosis. J Gastroenterol Hepatol 2010;25:613-8.
[32] Fan W, Boston BA, Kesterson RA, et al. Role of melanocortinergic neurons in feeding and the agouti obesity syndrome. Nature 1997;385:165-8.
[33] Huszar D, Lynch CA, Fairchild-Huntress V, et al. Targeted disruption of the melanocortin-4 receptor results in obesity in mice. Cell 1997;88:131-41.
[34] Cnop M, Ladrière L, Igoillo-Esteve M, et al. Causes and cures for endoplasmic reticulum stress in lipotoxic β-cell dysfunction. Diabetes Obes Metab 2010;12(Suppl 2):76-82.
[35] Seo HY, Kim MK, Min AK, et al. Endoplasmic reticulum stress-induced activation of activating transcription factor 6 decreases cAMP-stimulated hepatic gluconeogenesis via inhibition of CREB. Endocrinology 2010;151:561-8.
[36] Wang Y, Vera L, Fischer WH, et al. The CREB coactivator CRTC2 links hepatic ER stress and fasting gluconeogenesis. Nature 2009;460:534-7.
[37] Yamamoto K, Takahara K, Oyadomari S, et al. Induction of liver steatosis and lipid droplet formation in ATF6α-knockout mice burdened with pharmacological endoplasmic reticulum stress. Mol Biol Cell 2010;21:2975-86.
[38] Zeng L, Lu M, Mori K, et al. ATF6 modulates SREBP2-mediated lipogenesis. EMBO J 2004;23:950-8.
[39] Taniguchi A, Nakai Y, Sakai M, et al. Relationship of regional adiposity to insulin resistance and serum triglyceride levels in nonobese Japanese type 2 diabetes patioents. Metabolism 2002;51:544-8.
[40] Hollander WL, Bikman BT, Wang LP, et al. Lipid-induced insulin resistance mediated by the proinflammatory receptor TLR4 requires saturated fatty acid-induced ceramide biosynthesis in mice. J Clin Invest 2011;121:1858-70.

Please cite this article as: Usui M, et al, Atf6α-null mice are glucose intolerant due to pancreatic β-cell failure on a high-fat diet but partially resistant to diet-induced..., Metabolism (2012), doi:10.1016/j.metabol.2012.01.004

Open

Hypertension Research (2012) 35, 213–220

www.nature.com/hr

ORIGINAL ARTICLE

Modulation of renal superoxide dismutase by telmisartan therapy in C57BL/6-*Ins2*^{Akita} diabetic mice

Hiroki Fujita[1], Hiromi Fujishima[1], Tsukasa Morii[1], Takuya Sakamoto[2], Koga Komatsu[2], Mihoko Hosoba[1], Takuma Narita[1], Keiko Takahashi[3], Takamune Takahashi[3] and Yuichiro Yamada[1]

Renal superoxide excess, which is induced by an imbalance of the superoxide-producing enzyme NAD(P)H oxidase and the superoxide-scavenging enzyme superoxide dismutase (SOD) under hyperglycemia, increases oxidative stress and contributes to the development of diabetic nephropathy. In this study, we treated non-obese and hypoinsulinemic C57BL/6-*Ins2*^{Akita} (C57BL/6-Akita) diabetic mice with telmisartan (5 mg kg^{-1} per day), an angiotensin II type 1 receptor blocker, or amlodipine (5 mg kg^{-1} per day), a calcium channel blocker, for 4 weeks and compared the effects of these two anti-hypertensive drugs on renal NAD(P)H oxidase, SOD and transcription factor Nrf2 (NF-E2-related factor 2), which is known to upregulate several antioxidant enzymes including SOD. Vehicle-treated C57BL/6-Akita mice exhibited higher renal NAD(P)H oxidase and lower renal SOD activity with increased levels of renal superoxide than the C57BL/6-wild-type non-diabetic mice. Interestingly, telmisartan treatment not only reduced NAD(P)H oxidase activity but also enhanced SOD activity in C57BL/6-Akita mouse kidneys, leading to a reduction of renal superoxide levels. Furthermore, telmisartan-treated C57BL/6-Akita mice increased the renal protein expression of SOD and Nrf2. In parallel with the reduction of renal superoxide levels, a reduction of urinary albumin levels and a normalization of elevated glomerular filtration rate were observed in telmisartan-treated C57BL/6-Akita mice. In contrast, treatment with amlodipine failed to modulate renal NAD(P)H oxidase, SOD and Nrf2. Finally, treatment of C57BL/6-Akita mice with apocynin, an NAD(P)H oxidase inhibitor, also increased the renal protein expression of SOD and Nrf2. Collectively, our data suggest that NAD(P)H oxidase negatively regulates renal SOD, possibly by downregulation of Nrf2, and that telmisartan could upregulate renal SOD by the suppression of NAD(P)H oxidase and subsequent upregulation of Nrf2, leading to the amelioration of renal oxidative stress and diabetic renal changes.
Hypertension Research (2012) **35**, 213–220; doi:10.1038/hr.2011.176; published online 10 November 2011

Keywords: angiotensin II type 1 receptor blocker; diabetic nephropathy; NAD(P)H oxidase; superoxide dismutase; telmisartan

INTRODUCTION

Growing evidence indicates that superoxide anion ($O_2^{\bullet -}$) excess induced by chronic hyperglycemia contributes to glomerular injury, which characterizes diabetic nephropathy (DN) through the formation of secondary reactive oxygen species including peroxynitrite and hydroxyl radicals.[1–4] Two endogenous enzymes, NAD(P)H oxidase and superoxide dismutase (SOD), are thought to be key determinants for the superoxide anion levels in kidneys. NAD(P)H oxidase is the most important source of superoxide anions,[5–8] whereas SOD is a major defender against superoxide anions.[9,10] SOD consists of three enzymatic isoforms: cytosolic CuZn-SOD (SOD1), mitochondrial Mn-SOD (SOD2), and extracellular CuZn-SOD (SOD3).[10,11] These three isoforms are derived from distinct genes but catalyze the same reaction.[11] Each SOD isoform neutralizes superoxide anions into hydrogen peroxide (H_2O_2) and molecular oxygen,[9,10] followed by the reduction of hydrogen peroxide to water (H_2O) by catalase in peroxisomes or glutathione peroxidase in mitochondria.[1,12] Thus, SOD serves as a major antioxidant enzyme responsible for the first step of the superoxide removal system. Recent studies of streptozotocin-induced diabetic rats have shown that chronic hyperglycemia enhance NAD(P)H oxidase activity in kidneys.[4,13,14] Furthermore, we have more recently demonstrated that chronic hyperglycemia causes a reduction of renal SOD expression and activity in a mouse model susceptible to the development of DN.[15] On the basis of these findings, renal alterations of NAD(P)H oxidase and SOD enzymes are likely to be responsible for the renal superoxide excess observed in chronic hyperglycemia.

Angiotensin II is an important vasoconstrictor that regulates systemic and glomerular hemodynamics. In addition, angiotensin II is also known to promote sodium reabsorption, cell growth and extracellular matrix deposition in kidneys.[16] These effects are generally triggered by signaling via angiotensin II type 1 (AT1) receptors.[16] Therefore, AT1 receptor blockade not only improves systemic hypertension but also could provide direct renoprotective effects. Indeed,

[1]Division of Endocrinology, Metabolism and Geriatric Medicine, Akita University Graduate School of Medicine, Akita, Japan; [2]Division of Gastroenterology, Honjo Daiichi Hospital, Akita, Japan and [3]Division of Nephrology, Vanderbilt University Medical Center, Nashville, TN, USA
Correspondence: Dr H Fujita, Division of Endocrinology, Metabolism and Geriatric Medicine, Akita University Graduate School of Medicine, 1–1–1 Hondo, Akita 010-8543, Japan.
E-mail: hirofuji@gipc.akita-u.ac.jp
Received 10 March 2011; revised 21 July 2011; accepted 5 August 2011; published online 10 November 2011

AT1 receptor blockers (ARBs) have been shown to exert greater renoprotective effects in patients with DN than other classes of anti-hypertensive drugs. Clinical studies have reported that irbesartan, an ARB, significantly inhibits the aggravation of renal function in type 2 diabetic patients with overt DN compared with amlodipine,[17] a calcium channel blocker, and that valsartan, another ARB, significantly reduces albuminuria in type 2 diabetic patients with incipient DN compared with amlodipine.[18] It is noteworthy that the renoprotective effects of ARBs were independent of their systemic blood pressure-lowering properties. Recently, evidence for the anti-oxidative effects of ARBs has been accumulating for several members of the ARB class. Clinical studies have reported that ARBs, including losartan, candesartan, olmesartan, telmisartan and valsartan, reduce the urinary levels of oxidative stress marker 8-hydroxy-2′-deoxyguanosine in patients with DN.[19,20] Oxidative stress induced by superoxide excess under chronic hyperglycemia has been thought to be a major factor involved in the pathogenesis of DN.[21] Therefore, the powerful renoprotective properties of ARBs may be attributed to their antioxidative effects.

The role of angiotensin II in modulating superoxide-producing enzyme NAD(P)H oxidase has been explored in vascular cells and kidneys. Previous experimental studies have demonstrated that angiotensin II promotes superoxide generation via NAD(P)H oxidase activation in vascular cells.[22,23] Furthermore, recent experimental studies have indicated that ARBs, such as olmesartan and telmisartan, reduce glomerular superoxide production through downregulating the gene expression of NAD(P)H oxidase subunits p22*phox* and p47*phox* in subtotal nephrectomized rats[24] and catalase-deficient acatalasemic mice.[25] However, whether the angiotensin II signaling and its inhibition modulate the superoxide-scavenging SOD enzymes in kidneys exposed to hyperglycemia is largely unknown.

To investigate whether AT1 receptor blockade alters the expression and activity of SOD enzymes in kidneys exposed to hyperglycemia, we treated non-obese and hypoinsulinemic C57BL/6-*Ins2*^{Akita} (C57BL/6-Akita) diabetic mice with telmisartan, an ARB, or amlodipine, a calcium channel blocker, and compared the effects of these two anti-hypertensive drugs on renal SOD. We report here that telmisartan not only reduces renal NAD(P)H oxidase activity but also upregulates the renal expression and activity of SOD, resulting in a reduction of renal superoxide levels. To explore the mechanism underlying this upregulation of renal SOD with telmisartan, we further examined whether NAD(P)H oxidase inhibition with apocynin modulated the renal expression of SOD and redox-sensitive transcription factor Nrf2 (NF-E2-related factor 2), which is known to upregulate several antioxidant enzymes, including SOD,[26–28] in C57BL/6-Akita diabetic mice.

METHODS

Experimental animals

Male C57BL/6-Akita diabetic and C57BL/6-wild-type (C57BL/6-WT) non-diabetic mice were purchased from SLC (Shizuoka, Japan). The mice were housed (n=3–4 per cage) in a room with a relative humidity of 50% and a 12/12-h light/dark cycle at 20–22 °C, and had unrestricted access to standard rodent chow and water. Animal experiments were conducted in accordance with the Animal Welfare Guidelines of Akita University. All procedures were approved by the Committee on Animal Experimentation of Akita University.

Treatment protocols for telmisartan, amlodipine and apocynin

Telmisartan was kindly provided by Boehringer Ingelheim (Tokyo, Japan). Amlodipine, apocynin (4′-hydroxy-3′-methoxyacetophenone) and carboxymethylcellulose-Na were purchased from Sigma-Aldrich (St Louis, MO, USA). To investigate the effects of telmisartan and amlodipine on renal SOD and NAD(P)H oxidase, 10-week-old male C57BL/6-Akita diabetic mice were administered with telmisartan (5 mg kg^{-1}) orally or amlodipine (5 mg kg^{-1}) dissolved in a 0.5% carboxymethylcellulose-Na solution once daily for 4 weeks. Mice in the control group were given the same volume of 0.5% carboxymethylcellulose-Na solution alone as the vehicle. To examine the effects of NAD(P)H oxidase inhibition on renal SOD, 10-week-old male C57BL/6-Akita diabetic mice were treated with apocynin (40 mg kg^{-1} per day) for 8 weeks. Apocynin was added in the drinking water and was administered orally to the mice as described previously.[29] Mice in the control group were given water alone as the vehicle.

Measurement of blood and urine parameters

Blood glucose was measured using Glucocard Diameter (Arkray, Tokyo, Japan) on samples obtained after a 6-h daytime fast. Blood urea nitrogen, total plasma cholesterol and plasma triglycerides were enzymatically measured by an autoanalyzer (Fuji Dry-Chem 5500, Fuji Film, Tokyo, Japan). Urinary albumin excretion was assessed by determining the albumin-to-creatinine ratio in morning spot urine as previously described.[30] Urine albumin and creatinine were measured by an Albuwell-M Murine Microalbuminuria ELISA kit and a Creatinine Companion kit, respectively (Exocell, Philadelphia, PA, USA).

Measurement of physiological parameters and renal histologic analysis

Systolic blood pressure was measured in conscious trained mice at room temperature using a non-invasive tail cuff and a pulse transducer system (BP-98A, Softron, Tokyo, Japan). The glomerular filtration rate (GFR) was measured by a single-bolus fluorescein isothiocyanate-inulin injection method as described previously.[31] For renal histologic analysis, we stained kidney sections with periodic acid-Schiff (PAS). We used a semi-quantitative score to evaluate the degree and extent of glomerular mesangial expansion as described previously.[30]

Renal superoxide production and activity of NAD(P)H oxidase and SOD

Renal superoxide levels were assessed by dihydroethidium (DHE) histochemistry and a water-soluble tetrazolium salt (WST-1, 2-[4-iodophenyl]-3-[4-nitrophenyl]-5-[2,4-disulfophenyl]-2H-tetrazolium) reduction assay as previously described.[15] The specificity of the WST-1 assay was confirmed by pretreating 10 mg of kidney tissue with polyethylene glycol-SOD (20U; Sigma-Aldrich) overnight at 37 °C. Renal superoxide levels were expressed as the absorbance at 450 nm per 10 mg tissue. For the DHE staining, we examined the Eth-DNA fluorescence at 480 nm excitation and 610 nm emission. To measure renal NAD(P)H oxidase and SOD activity, we prepared kidney lysates using phosphate-buffered saline-perfused and freshly removed renal cortical tissue as previously described.[15] Renal NAD(P)H oxidase activity was measured by a lucigenin-enhanced chemiluminescence assay as previously described.[14] Renal SOD activity was determined using an SOD assay kit-WST (Dojindo Molecular Technologies, Gaithersburg, MD, USA) as previously described.[15] The protein amount was measured using a bicinochoninic acid protein assay (Sigma-Aldrich). The enzymatic activity of NAD(P)H and SOD were expressed in relative chemiluminescence (light) units (RLU) per 100 μg protein and units per mg protein, respectively.

Western blot analysis and immunohistochemistry

For western blot analysis, the kidney lysate prepared for the SOD activity measurement was used. In all, 20 μg of protein was separated by SDS-PAGE and subjected to immunoblots. As the primary antibody, we used rabbit anti-CuZn-SOD (SOD1) (1 : 10 000; Stressgen, Ann Arbor, MI, USA), anti-Mn-SOD (SOD2) (1 : 10 000; Stressgen), anti-EC-SOD (SOD3) (1 : 2000; Stressgen) or anti-Nrf2 (1 : 1000; Santa Cruz Biotechnology, Santa Cruz, CA, USA) polyclonal antibodies. The loading of lysate protein was evaluated by an immunoblot using rabbit anti-actin antibody (1 : 1000; Sigma-Aldrich). The intensity of the signals was semi-quantified using Adobe Photoshop (version CS4; Adobe Systems, San Jose, CA, USA). For the immunohistochemistry, cryostat sections were prepared as previously described.[15] We labeled the sections with rabbit

Table 1 Physiological and biochemical parameters after 4-week treatment with amlodipine or telmisartan in C57BL/6-Akita diabetic mice

	C57BL/6-WT	*C57BL/6-Akita*		
Parameter	*No treatment*	*Vehicle*	*Amlodipine*	*Telmisartan*
n	8	6	6	8
Body weight (g)	23.6 ± 0.7	20.6 ± 0.6*	19.9 ± 0.4*	20.6 ± 0.5*
Systolic blood pressure (mm Hg)	99 ± 2	116 ± 5*	103 ± 2‡	102 ± 3‡
Blood glucose (mg dl^{-1})	148 ± 8	463 ± 18†	429 ± 19†	447 ± 18†
BUN (mg dl^{-1})	23.6 ± 0.7	32.5 ± 1.9*	33.2 ± 1.9*	32.5 ± 2.2*
Total cholesterol (mg dl^{-1})	76.8 ± 3.6	82.6 ± 2.0	84.8 ± 6.8	82.7 ± 3.4
Triglyceride (mg dl^{-1})	75.0 ± 4.4	75.0 ± 4.3	72.7 ± 3.1	69.6 ± 4.7
Urinary albumin (μg per mg creatinine)	9.4 ± 4.8	59.2 ± 6.7†	56.9 ± 5.6†	28.6 ± 3.9§
GFR (ml min^{-1} per g BW)	10.0 ± 0.5	16.3 ± 1.1†	16.7 ± 0.9†	12.7 ± 0.4‡
LKW/BW (g kg^{-1})	7.2 ± 0.3	11.5 ± 0.4†	11.9 ± 0.5†	9.4 ± 0.2†,§
Mesangial expansion score	0.15 ± 0.01	0.44 ± 0.03†	0.41 ± 0.05†	0.40 ± 0.03†

Abbreviations: BUN, blood urea nitrogen; BW, body weight; GFR, glomerular filtration rate; LKW, left kidney weight.
Values are means ± s.e.m. *$P<0.01$, †$P<0.001$ *vs.* C57BL/6-WT. ‡$P<0.05$, §$P<0.01$ *vs.* vehicle.

anti-CuZn-SOD (SOD1) (1 : 100; Stressgen), anti-Mn-SOD (SOD2) (1 : 100; Stressgen) or anti-EC-SOD (SOD3) (1 : 50; Stressgen) polyclonal antibodies for 1 h at room temperature, followed by Alexa Fluor 488-conjugated goat anti-rabbit IgG antibody (1 : 200; Molecular Probes, Eugene, OR, USA) for 30 min at room temperature. We then counterstained the sections with ToPro-3 (Molecular Probes).

Measurement of renal prostaglandin E2 (PGE2) levels

Renal PGE2 levels were measured using freshly isolated renal cortical tissue as previously described.[32] The levels were expressed as the ratio of renal cortical PGE2 to protein.

Statistical analysis

Data were presented as the mean ± s.e.m. Statistical analyses were conducted using GraphPad Prism software (GraphPad, San Diego, CA, USA). Differences between groups were determined by an unpaired *t*-test or a one-way ANOVA, followed by Bonferroni's multiple comparison test. A $P<0.05$ was considered statistically significant.

RESULTS

Biochemical and physiological parameters, and renal histopathology after a 4-week treatment with telmisartan or amlodipine in C57BL/6-Akita diabetic mice

Table 1 shows the biochemical and physiological parameters after a 4-week treatment with telmisartan or amlodipine in C57BL/6-Akita diabetic mice. Data from telmisartan-treated mice were compared with those from the mice treated with amlodipine. Treatment with either telmisartan or amlodipine did not affect blood glucose, body weight, blood urea nitrogen, total cholesterol or triglyceride levels. Compared with the vehicle-treated mice, both amlodipine-treated and telmisartan-treated mice exhibited significantly lower blood pressure levels. There were no significant differences in blood pressure levels between amlodipine-treated and telmisartan-treated mice. Compared with the data from vehicle-treated mice, treatment with telmisartan significantly reduced urinary albumin levels, GFR, and the left kidney weight-to-body weight ratio (LKW/BW) in C57BL/6-Akita diabetic mice, whereas treatment with amlodipine had no effect. As we recently reported, glomerular pathological damages were relatively mild in 10–15-week-old C57BL/6-Akita diabetic mice.[15] A difference in glomerular pathological changes evaluated using the mesangial expansion score was not observed between vehicle-treated and telmisartan-treated C57BL/6-Akita diabetic mice.

Effects of treatment with telmisartan on renal superoxide production, NAD(P)H oxidase activity and SOD activity in C57BL/6-Akita diabetic mice

Figure 1 shows renal superoxide production, NAD(P)H oxidase activity and SOD activity after a 4-week treatment with telmisartan or amlodipine in C57BL/6-Akita diabetic mice. Renal superoxide levels were assessed by DHE histochemistry and a WST-1 assay. The DHE fluorescence signal, which reflects superoxide production, was decreased in the glomeruli of telmisartan-treated C57BL/6-Akita diabetic mice compared with vehicle-treated mice (Figure 1A). Furthermore, telmisartan but not amlodipine significantly reduced renal superoxide levels as determined by the WST-1 assay in C57BL/6-Akita diabetic mice (Figure 1B). Consistent with a recent report,[33] telmisartan reduced NAD(P)H activity in the kidneys of C57BL/6-Akita diabetic mice close to the levels of C57BL/6-wild-type (C57BL/6-WT) non-diabetic mice (Figure 1C). Interestingly, telmisartan-treated C57BL/6-Akita diabetic mice but not amlodipine-treated mice showed significantly higher renal SOD activity than the vehicle-treated mice (Figure 1D). Thus, it should be noted that two telmisartan-treated and amlodipine-treated C57BL/6-Akita diabetic mouse groups exhibited different levels of renal NAD(P)H and SOD activity, despite comparable levels of hyperglycemia and blood pressure.

Effects of treatment with telmisartan on the renal expression of SOD isoforms and Nrf2 in C57BL/6-Akita diabetic mice

We next examined whether a 4-week treatment with telmisartan affected the renal expression of SOD isoforms and Nrf2. Western blot analysis revealed increased expression of the SOD isoforms SOD1, SOD2, and SOD3 and Nrf2 in the renal cortex of telmisartan-treated C57BL/6-Akita diabetic mice, whereas renal SOD and Nrf2 upregulation was not observed in amlodipine-treated mice (Figure 2). Figure 3 shows the renal SOD isoform expression using immunofluorescence histochemistry. As shown in our recent report,[15] SOD1 and SOD2 were broadly expressed in glomerular and tubular cells (tubular SOD1 expression not shown). SOD3 expression was observed in glomerular capillaries and the arteriolar wall (expression of SOD3 in the arteriolar wall not shown). Consistent with the results of the western blot analysis, strong SOD1 and SOD3 signals in the glomeruli and SOD2 signals in proximal tubules were observed in telmisartan-treated C57BL/6-Akita diabetic mice.

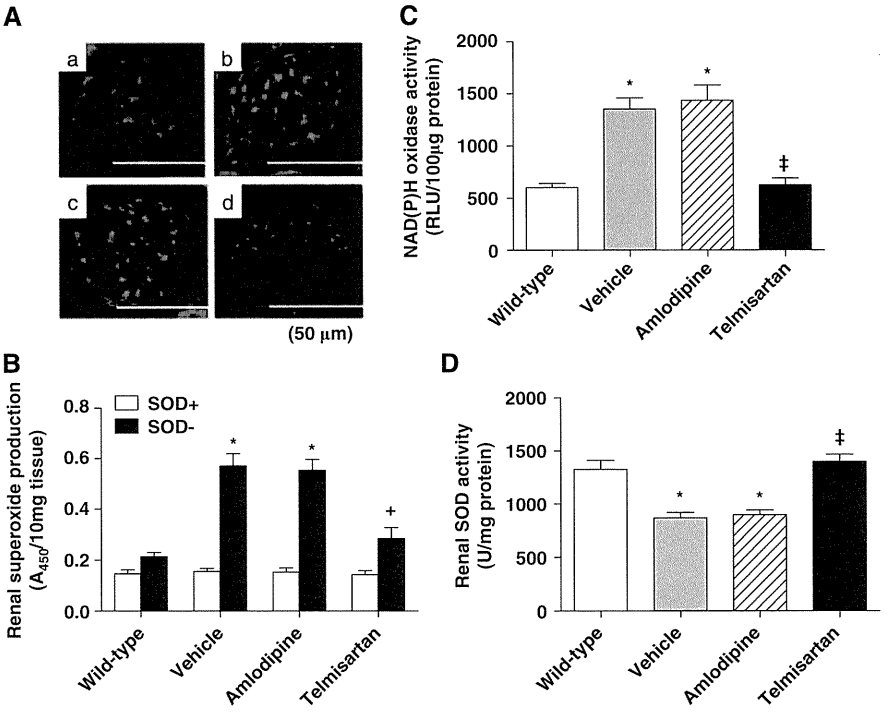

Figure 1 Effects of telmisartan treatment on renal superoxide production, NAD(P)H oxidase activity and SOD activity in C57BL/6-Akita diabetic mice. The C57BL/6-Akita diabetic mice were treated with the vehicle, amlodipine or telmisartan for 4 weeks. The treatment started at 10 weeks of age and ended at 14 weeks of age. The data from C57BL/6-Akita diabetic mice were compared with those from age-matched C57BL/6-wild-type non-diabetic mice. (**A**) Representative glomerular DHE staining after a 4-week treatment with telmisartan. (a) C57BL/6-wild-type; (b) vehicle-treated C57BL/6-Akita; (c) amlodipine-treated C57BL/6-Akita; (d) telmisartan-treated C57BL/6-Akita. (**B**) Renal superoxide production after a 4-week treatment with telmisartan. Data are presented as the mean ± s.e.m. SOD+, kidney tissue pre-incubated with SOD-PEG protein; SOD−, kidney tissue without SOD-PEG protein. n=5 per group. $^{*}P<0.001$ *vs.* wild-type. $^{+}P<0.01$ *vs.* vehicle. (**C**) Renal NAD(P)H oxidase activity after a 4-week treatment with telmisartan. Data are presented as the mean ± s.e.m. n=5 per group. $^{*}P<0.001$ *vs.* wild-type. $^{\ddagger}P<0.001$ *vs.* vehicle. (**D**) Renal SOD activity after a 4-week treatment with telmisartan. Data are presented as the mean ± s.e.m. n=5 per group. $^{*}P<0.001$ *vs.* wild-type. $^{\ddagger}P<0.001$ *vs.* vehicle.

In contrast, the kidneys of amlodipine-treated C57BL/6-Akita diabetic mice did not exhibit increased expression of SOD isoforms.

NAD(P)H oxidase inhibition by treatment with apocynin and renal alterations of the SOD enzyme and Nrf2 in C57BL/6-Akita diabetic mice

We found that telmisartan reduced renal superoxide levels through downregulating NAD(P)H oxidase and upregulating SOD in a mouse model of diabetes, C57BL/6-Akita mice. To explore whether NAD(P)H oxidase regulates the SOD enzyme via Nrf2 in kidneys, we treated C57BL/6-Akita diabetic mice with apocynin, an NAD(P)H oxidase inhibitor, for 8 weeks and investigated the renal alterations of the SOD enzyme and Nrf2. As shown in Table 2, apocynin treatment did not affect body weight, blood pressure, blood glucose or LKW/BW. As expected, a marked reduction of renal superoxide and NAD(P)H oxidase activity was observed in the apocynin-treated C57BL/6-Akita diabetic mice. In addition, apocynin significantly lowered urinary albumin levels and ameliorated elevated GFR in C57BL/6-Akita diabetic mice. Figure 4 shows the western blot analysis of renal cortical expression of SOD isoforms and Nrf2 after an 8-week treatment with apocynin. Interestingly, renal cortical expression levels of SOD1, SOD2 and SOD3 isoforms and Nrf2 were significantly increased in apocynin-treated C57BL/6-Akita diabetic mice compared with vehicle-treated mice.

Effects of telmisartan and apocynin on renal production of vasodilatory PGE2 in C57BL/6-Akita diabetic mice

To elucidate the mechanism through which superoxide reduction due to treatment with telmisartan or apocynin affects glomerular hemodynamics, we measured renal cortical levels of vasodilatory PGE2, which contributes to the development of glomerular hypertension in C57BL/6-Akita diabetic mouse groups treated with telmisartan for 4 weeks and with apocynin for 8 weeks. As shown in Figure 5, a reduction of renal PGE2 production was observed in the telmisartan-treated and apocynin-treated groups compared with the vehicle-treated group.

DISCUSSION

Telmisartan is a unique ARB with peroxisome proliferator-activated receptor-γ activity,[34] and this ARB has been reported to offer a more powerful antioxidative effect than other members of the ARB class in patients with DN.[20] In this study, we first treated 10-week-old C57BL/6-Akita diabetic mice with telmisartan for 4 weeks and investigated whether AT1 receptor blockade by telmisartan modulated the superoxide-scavenging SOD enzyme in kidneys exposed to hyperglycemia. C57BL/6-Akita mice are well-characterized as a model of non-obese and hypoinsulinemic diabetes, and develop marked hyperglycemia as early as 4 weeks of age because of a single mutation in cysteine 96 to tyrosin in the insulin 2 gene (*Ins2*^{Akita}).[35,36] Chemicals such as streptozotocin or alloxan are widely used to induce diabetes in

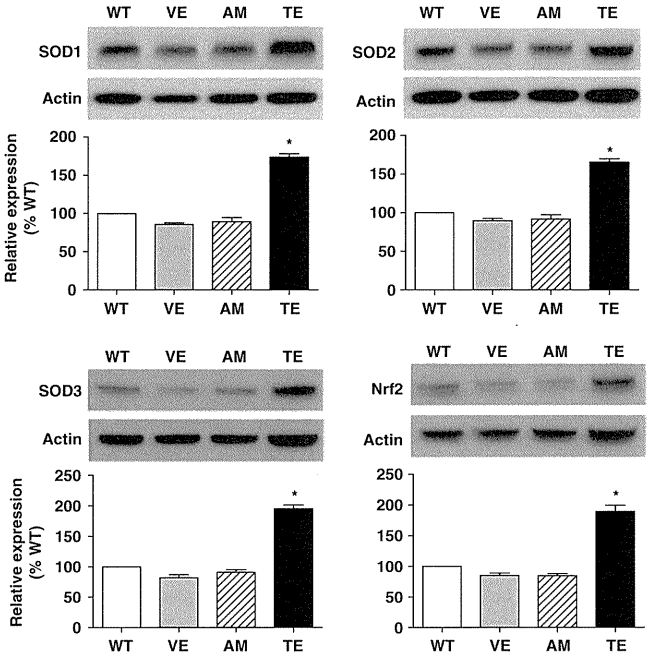

Figure 2 Western blot analysis of renal cortical SOD isoforms and Nrf2 expression after a 4-week treatment with the vehicle (VE), amlodipine (AM) or telmisartan (TE) in C57BL/6-Akita diabetic mice. WT indicates non-diabetic C57BL/6-wild-type mice. The relative intensity of the SOD-to-actin or Nrf2-to-actin ratios to WT is also shown in the lower panels. Data are presented as the mean ± s.e.m. n=4 per group. $^{*}P<0.001$ *vs.* VE.

experimental animals. However, these chemicals have been documented to generate reactive oxygen species and enhance oxidative stress.[37] Therefore, the C57BL/6-Akita mouse model offers a unique opportunity to precisely assess the renal alterations of oxidative stress and its related enzymes.

Consistent with the results of clinical studies,[17,18] our data also indicate that an ARB, telmisartan, is superior to a calcium channel blocker, amlodipine, at producing renoprotective effects in C57BL/6-

Table 2 Physiological and biochemical parameters after 8-week treatment with apocynin in C57BL/6-Akita diabetic mice

Parameter	*Vehicle*	*Apocynin*
n	5	5
Body weight (g)	23.0 ± 0.4	23.4 ± 0.4
Systolic blood pressure (mm Hg)	116 ± 2	115 ± 4
Blood glucose (mg dl^{-1})	466 ± 18	474 ± 7
Urinary albumin (μg per mg creatinine)	66.4 ± 5.8	32.7 ± 4.6*
GFR (ml min^{-1} per g BW)	16.9 ± 0.8	12.2 ± 0.7*
LKW/BW (g kg^{-1})	10.3 ± 0.5	9.3 ± 0.4
Renal superoxide (A_{450}/10 mg tissue)	0.609 ± 0.023	0.244 ± 0.023†
Renal NAD(P)H oxidase activity (RLU per 100 μg protein)	1236 ± 16	315 ± 20†
Renal SOD activity (U mg^{-1} protein)	824 ± 34	1285 ± 78†

Abbreviations: BW, body weight; GFR, glomerular filtration rate; LKW, left kidney weight; RLU, relative light units; SOD, superoxide dismutase.
Values are means ± s.e.m. *P<0.01, †P<0.001 *vs.* vehicle.

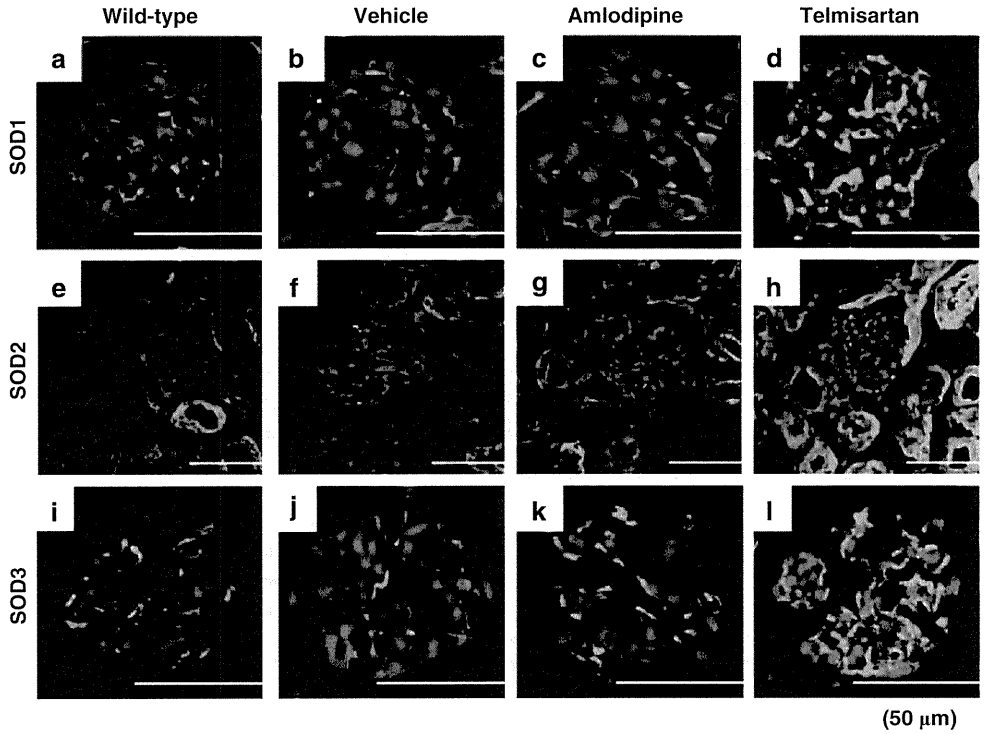

Figure 3 Immunofluorescence SOD isoform staining of kidney sections after a 4-week treatment with the vehicle, amlodipine or telmisartan in C57BL/6-Akita diabetic mice. (**a–d**) SOD1; (**e–h**) SOD2; (**i–l**) SOD3; (**a**, **e**, **i**) C57BL/6-wild-type; (**b**, **f**, **j**) vehicle-treated C57BL/6-Akita; (**c**, **g**, **k**) amlodipine-treated C57BL/6-Akita; (**d**, **h**, **l**) telmisartan-treated C57BL/6-Akita.

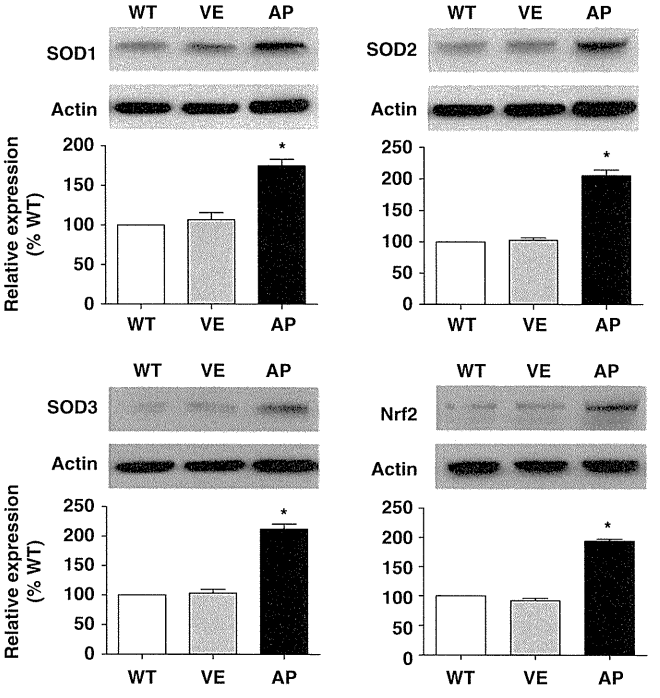

Figure 4 Western blot analysis of renal cortical SOD isoform and Nrf2 expression after an 8-week treatment with the vehicle (VE) or apocynin (AP) in C57BL/6-Akita diabetic mice. WT indicates non-diabetic C57BL/6-wild-type mice. The relative intensity of the SOD-to-actin or Nrf2-to-actin ratios to WT is also shown in the lower panels. Data are presented as the mean ± s.e.m. n=4 per group. $^{*}P<0.001$ *vs.* VE.

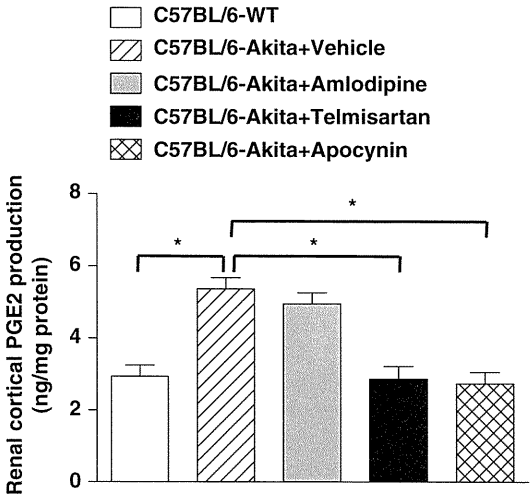

Figure 5 Renal cortical PGE2 levels after a 4-week treatment with the vehicle, amlodipine or telmisartan and after an 8-week treatment with apocynin in C57BL/6-Akita diabetic mice. Data are presented as the mean ± s.e.m. n=5 per group. $^{*}P<0.001$.

Akita diabetic mice. In the SMART study, it was reported that changes in the urinary albumin-to-creatinine ratio from baseline to the end of the treatment period were −36% in type 2 diabetic and microalbuminuric patients treated with valsartan, an ARB, for 24 weeks and +30% in those treated with amlodipine for 24 weeks, despite comparable blood pressure reductions.[38] These results indicate that monotherapy with amlodipine may be insufficient for albumin-to-creatinine ratio reduction. However, the SMART study also suggested that if blood pressure is sufficiently lowered by amlodipine treatment, albumin-to-creatinine ratio would also be reduced to some extent. Similar to the results of the SMART study, this study showed that treatment with telmisartan, not amlodipine, reduced urinary albumin levels and normalized elevated GFR that reflects glomerular hypertension in C57BL/6-Akita diabetic mice, despite comparable levels of hyperglycemia and blood pressure between the two groups treated with these drugs. Further blood pressure reduction with amlodipine treatment may be needed to reduce urinary albumin and glomerular hypertension in C57BL/6-Akita diabetic mice.

In this study, we used the tail cuff method to measure blood pressure. Our data did not indicate a difference in blood pressure between the telmisartan-treated and amlodipine-treated C57BL/6-Akita diabetic mice. However, the tail cuff method has several limitations in blood pressure measurement. Therefore, measuring blood pressure with the telemetry method may be necessary to precisely assess the effects of anti-hypertensive drugs on reducing blood pressure in C57BL/6-Akita diabetic mice.

Our experiments revealed the novel finding that telmisartan not only reduced NAD(P)H oxidase activity but also enhanced SOD activity in the kidneys of C57BL/6-Akita diabetic mice. As expected, renal alterations of these enzymes resulted in a reduction of renal superoxide levels. In contrast, treatment with amlodipine failed to modulate renal NAD(P)H oxidase and SOD enzymes. The differences in renoprotection between telmisartan and amlodipine may in part be attributed to their ability to modulate renal NAD(P)H oxidase and SOD enzymes. A recent experimental study reported that treatment with low doses of telmisartan (0.1–0.3 mg kg^{-1} per day) did not affect renal SOD activity in non-diabetic mice.[25] However, our study indicated that treatment with a high dose of telmisartan (5 mg kg^{-1} per day) enhanced renal SOD activity in C57BL/6-Akita diabetic mice. It is possible that high doses of this ARB are needed to enhance renal SOD activity. Paralleling the elevation of renal SOD activity in telmisartan-treated C57BL/6-Akita diabetic mice, our immunohistochemical study revealed increases in the protein expression of SOD1 and SOD3 isoforms in glomeruli and of the SOD2 isoform in the proximal tubules of these mice. Western blot analysis confirmed the finding that telmisartan therapy increases the protein expression of SOD1, SOD2 and SOD3 in the kidneys of C57BL/6-Akita diabetic mice.

As angiotensin II signaling directly promotes NAD(P)H oxidase activation,[22,23] the downregulation of renal NAD(P)H oxidase by AT1 receptor blockade is a reasonable result. However, the mechanism by which telmisartan upregulates renal SOD remains unclear. We hypothesized that NAD(P)H oxidase would negatively regulate the renal expression of SOD or transcription factor Nrf2, which is known to upregulate several antioxidant enzymes including SOD.[26–28] To test this hypothesis, we treated C57BL/6-Akita diabetic mice with an NAD(P)H oxidase inhibitor, apocynin, for 8 weeks and investigated the alteration of renal SOD and Nrf2 expression. As expected, apocynin treatment markedly lowered renal NAD(P)H oxidase activity in C57BL/6-Akita diabetic mice, resulting in the reduction of renal superoxide levels. The reduction of renal superoxide by apocynin therapy contributed to reducing urinary albumin levels and normalizing the elevated GFR in C57BL/6-Akita diabetic mice. Consistent with the results of recent experimental studies,[29,39] apocynin did not lower the blood pressure of C57BL/6-Akita diabetic mice. Although the cause is unclear, one possible explanation is that unlike telmisartan, apocynin is not effective in blocking systemic vasoconstriction by angiotensin II. More importantly, we found that inhibiting NAD(P)H

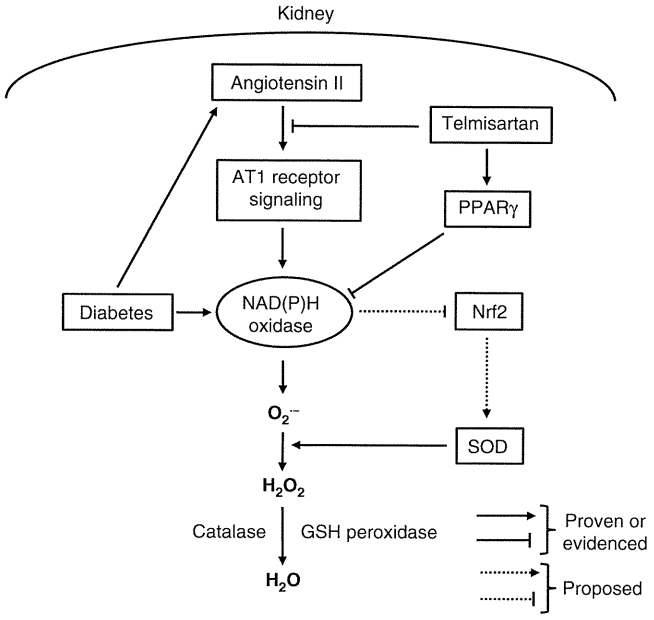

Figure 6 The proposed mechanism by which telmisartan upregulates renal SOD in diabetes.

oxidase upregulated renal SOD and Nrf2 in C57BL/6-Akita diabetic mice. Suppression of NAD(P)H oxidase by telmisartan also resulted in increased expression of renal Nrf2. Taken together, our data suggest that NAD(P)H oxidase negatively regulates renal SOD, possibly by downregulation of Nrf2, and that telmisartan could upregulate renal SOD by the suppression of NAD(P)H oxidase and subsequent upregulation of Nrf2 (Figure 6).

This study does not demonstrate that other members of the ARB class also have the ability to upregulate renal SOD. As AT1 receptor blockade by other members of the ARB class, such as olmesartan, has been shown to reduce renal NAD(P)H oxidase expression,[24] all ARBs may share the renal SOD upregulating effect to some extent. However, as shown in a recent clinical study,[20] there is a difference in the ability to ameliorate oxidative stress among the ARB members. Of the currently available ARBs, telmisartan is known to have the strongest binding affinity to AT1 receptors, the longest half-life, and a high lipophilicity.[40,41] In addition, telmisartan also acts as a partial agonist of peroxisome proliferator-activated receptor-γ. An experimental study of obese and hypertensive rats has indicated that peroxisome proliferator-activated receptor-γ activation by pioglitazone therapy downregulates NAD(P)H oxidase.[42] These properties may explain the more powerful antioxidative and renoprotective effects of telmisartan by modulation of renal NAD(P)H oxidase and SOD.

Reactive oxygen species, including superoxide anions, induce overproduction of vasodilatory PGE2 through cyclooxygenase-2 upregulation.[43] PGE2 is a vasodilator for afferent arterioles, and excessive PGE2 could cause the glomerular hypertension observed in early diabetes.[44,45] Therefore, it is thought that the reduction of renal superoxide with apocynin normalized elevated GFR in C57BL/6-Akita diabetic mice. In addition, renal superoxide reduction with telmisartan is likely to affect glomerular pressure reduction. This study revealed that treatment with apocynin or telmisartan reduces renal PGE2 production in C57BL/6-Akita diabetic mice. Furthermore, the ability of telmisartan to dilate efferent arterioles through AT1 receptor blockade also contributes to the amelioration of glomerular hypertension. Thus, renal superoxide reduction is thought to provide beneficial effects in improving abnormalities in glomerular hemodynamics in early diabetes.

In conclusion, we report a novel finding that AT1 receptor blockade by telmisartan treatment could upregulate renal SOD enzyme by the suppression of NAD(P)H oxidase and subsequent upregulation of Nrf2, leading to an improvement of oxidative stress in kidneys exposed to hyperglycemia. These effects are expected to greatly contribute to the amelioration of earlier diabetic renal change observed in C57BL/6-Akita diabetic mice.

CONFLICTS OF INTEREST

The authors declare no conflict of interest.

ACKNOWLEDGEMENTS

This work was supported by a Grant-in-Aid for Scientific Research (No. 20590943 and No. 23591177, to H Fujita) from the Ministry of Education, Science and Culture, Japan.

1 Evans JL, Goldfine ID, Maddux BA, Grodsky GM. Oxidative stress and stress-activated signaling pathways: a unifying hypothesis of type 2 diabetes. *Endocr Rev* 2002; **23**: 599–622.
2 Coughlan MT, Thorburn DR, Penfold SA, Laskowski A, Harcourt BE, Sourris KC, Tan AL, Fukami K, Thallas-Bonke V, Nawroth PP, Brownlee M, Bierhaus A, Cooper ME, Forbes JM. RAGE-induced cytosolic ROS promote mitochondrial superoxide generation in diabetes. *J Am Soc Nephrol* 2009; **20**: 742–752.
3 Ghosh S, Khazaei M, Moien-Afshari F, Ang LS, Granville DJ, Verchere CB, Dunn SR, McCue P, Mizisin A, Sharma K, Laher I. Moderate exercise attenuates caspase-3 activity, oxidative stress, and inhibits progression of diabetic renal disease in db/db mice. *Am J Physiol Renal Physiol* 2009; **296**: F700–F708.
4 Thallas-Bonke V, Thorpe SR, Coughlan MT, Fukami K, Yap FY, Sourris KC, Penfold SA, Bach LA, Cooper ME, Forbes JM. Inhibition of NADPH oxidase prevents advanced glycation end product-mediated damage in diabetic nephropathy through a protein kinase C-alpha-dependent pathway. *Diabetes* 2008; **57**: 460–469.
5 Guzik TJ, Mussa S, Gastaldi D, Sadowski J, Ratnatunga C, Pillai R, Channon KM. Mechanisms of increased vascular superoxide production in human diabetes mellitus: role of NAD(P)H oxidase and endothelial nitric oxide synthase. *Circulation* 2002; **105**: 1656–1662.
6 Satoh M, Fujimoto S, Haruna Y, Arakawa S, Horike H, Komai N, Sasaki T, Tsujioka K, Makino H, Kashihara N. NAD(P)H oxidase and uncoupled nitric oxide synthase are major sources of glomerular superoxide in rats with experimental diabetic nephropathy. *Am J Physiol Renal Physiol* 2005; **288**: F1144–F1152.
7 Soccio M, Toniato E, Evangelista V, Carluccio M, De Caterina R. Oxidative stress and cardiovascular risk: the role of vascular NAD(P)H oxidase and its genetic variants. *Eur J Clin Invest* 2005; **35**: 305–314.
8 Wardle EN. Cellular oxidative processes in relation to renal disease. *Am J Nephrol* 2005; **25**: 13–22.
9 Fridovich I. Superoxide radical and superoxide dismutases. *Annu Rev Biochem* 1995; **64**: 97–112.
10 Fridovich I. Superoxide anion radical ($O_2^{\bullet-}$). *J Biol Chem* 1997; **272**: 18515–18517.
11 Faraci FM, Didion SP. Vascular protection: superoxide dismutase isoforms in the vessel wall. *Arterioscler Thromb Vasc Biol* 2004; **24**: 1367–1373.
12 Son SM. Role of vascular reactive oxygen species in development of vascular abnormalities in diabetes. *Diabetes Res Clin Pract* 2007; **77**(Suppl 1): S65–S70.
13 Gorin Y, Block K, Hernandez J, Bhandari B, Wagner B, Barnes JL, Abboud HE. Nox4 NAD(P)H oxidase mediates hypertrophy and fibronectin expression in the diabetic kidney. *J Biol Chem* 2005; **280**: 39616–39626.
14 Kitada M, Koya D, Sugimoto T, Isono M, Araki S, Kashiwagi A, Haneda M. Translocation of glomerular p47phox and p67phox by protein kinase C-beta activation is required for oxidative stress in diabetic nephropathy. *Diabetes* 2003; **52**: 2603–2614.
15 Fujita H, Fujishima H, Chida S, Takahashi K, Qi Z, Kanetsuna Y, Breyer MD, Harris RC, Yamada Y, Takahashi T. Reduction of renal superoxide dismutase in progressive diabetic nephropathy. *J Am Soc Nephrol* 2009; **20**: 1303–1313.
16 Ram CV. Angiotensin receptor blockers: current status and future prospects. *Am J Med* 2008; **121**: 656–663.
17 Lewis EJ, Hunsicker LG, Clarke WR, Berl T, Pohl MA, Lewis JB, Ritz E, Atkins RC, Rohde R, Raz I. Renoprotective effect of the angiotensin-receptor antagonist irbesartan in patients with nephropathy due to type 2 diabetes. *N Engl J Med* 2001; **345**: 851–860.
18 Viberti G, Wheeldon NM. Microalbuminuria reduction with valsartan in patients with type 2 diabetes mellitus: a blood pressure-independent effect. *Circulation* 2002; **106**: 672–678.
19 Ogawa S, Mori T, Nako K, Kato T, Takeuchi K, Ito S. Angiotensin II type 1 receptor blockers reduce urinary oxidative stress markers in hypertensive diabetic nephropathy. *Hypertension* 2006; **47**: 699–705.

20 Nakamura T, Fujiwara N, Sato E, Ueda Y, Sugaya T, Koide H. Renoprotective effects of various angiotensin II receptor blockers in patients with early-Stage diabetic nephropathy. *Kidney Blood Press Res* 2010; **33**: 213–220.
21 Brownlee M. The pathobiology of diabetic complications: a unifying mechanism. *Diabetes* 2005; **54**: 1615–1625.
22 Rajagopalan S, Kurz S, Munzel T, Tarpey M, Freeman BA, Griendling KK, Harrison DG. Angiotensin II-mediated hypertension in the rat increases vascular superoxide production via membrane NADH/NADPH oxidase activation. Contribution to alterations of vasomotor tone. *J Clin Invest* 1996; **97**: 1916–1923.
23 Griendling KK, Minieri CA, Ollerenshaw JD, Alexander RW. Angiotensin II stimulates NADH and NADPH oxidase activity in cultured vascular smooth muscle cells. *Circ Res* 1994; **74**: 1141–1148.
24 Fujimoto S, Satoh M, Horike H, Hatta H, Haruna Y, Kobayashi S, Namikoshi T, Arakawa S, Tomita N, Kashihara N. Olmesartan ameliorates progressive glomerular injury in subtotal nephrectomized rats through suppression of superoxide production. *Hypertens Res* 2008; **31**: 305–313.
25 Sugiyama H, Kobayashi M, Wang DH, Sunami R, Maeshima Y, Yamasaki Y, Masuoka N, Kira S, Makino H. Telmisartan inhibits both oxidative stress and renal fibrosis after unilateral ureteral obstruction in acatalasemic mice. *Nephrol Dial Transplant* 2005; **20**: 2670–2680.
26 Negi G, Kumar A, Joshi RP, Sharma SS. Oxidative stress and Nrf2 in the pathophysiology of diabetic neuropathy: old perspective with a new angle. *Biochem Biophys Res Commun* 2011; **408**: 1–5.
27 Chan K, Kan YW. Nrf2 is essential for protection against acute pulmonary injury in mice. *Proc Natl Acad Sci USA* 1999; **96**: 12731–12736.
28 Chan K, Han XD, Kan YW. An important function of Nrf2 in combating oxidative stress: detoxification of acetaminophen. *Proc Natl Acad Sci USA* 2001; **98**: 4611–4616.
29 Schluter T, Steinbach AC, Steffen A, Rettig R, Grisk O. Apocynin-induced vasodilation involves Rho kinase inhibition but not NADPH oxidase inhibition. *Cardiovasc Res* 2008; **80**: 271–279.
30 Qi Z, Fujita H, Jin J, Davis LS, Wang Y, Fogo AB, Breyer MD. Characterization of susceptibility of inbred mouse strains to diabetic nephropathy. *Diabetes* 2005; **54**: 2628–2637.
31 Qi Z, Whitt I, Mehta A, Jin J, Zhao M, Harris RC, Fogo AB, Breyer MD. Serial determination of glomerular filtration rate in conscious mice using FITC-inulin clearance. *Am J Physiol Renal Physiol* 2004; **286**: F590–F596.
32 Fujita H, Kakei M, Fujishima H, Morii T, Yamada Y, Qi Z, Breyer MD. Effect of selective cyclooxygenase-2 (COX-2) inhibitor treatment on glucose-stimulated insulin secretion in C57BL/6 mice. *Biochem Biophys Res Commun* 2007; **363**: 37–43.
33 Takaya T, Kawashima S, Shinohara M, Yamashita T, Toh R, Sasaki N, Inoue N, Hirata K, Yokoyama M. Angiotensin II type 1 receptor blocker telmisartan suppresses superoxide production and reduces atherosclerotic lesion formation in apolipoprotein E-deficient mice. *Atherosclerosis* 2006; **186**: 402–410.
34 Benson SC, Pershadsingh HA, Ho CI, Chittiboyina A, Desai P, Pravenec M, Qi N, Wang J, Avery MA, Kurtz TW. Identification of telmisartan as a unique angiotensin II receptor antagonist with selective PPARgamma-modulating activity. *Hypertension* 2004; **43**: 993–1002.
35 Yoshioka M, Kayo T, Ikeda T, Koizumi A. A novel locus, Mody4, distal to D7Mit189 on chromosome 7 determines early-onset NIDDM in nonobese C57BL/6 (Akita) mutant mice. *Diabetes* 1997; **46**: 887–894.
36 Wang J, Takeuchi T, Tanaka S, Kubo SK, Kayo T, Lu D, Takata K, Koizumi A, Izumi T. A mutation in the insulin 2 gene induces diabetes with severe pancreatic beta-cell dysfunction in the Mody mouse. *J Clin Invest* 1999; **103**: 27–37.
37 Szkudelski T. The mechanism of alloxan and streptozotocin action in B cells of the rat pancreas. *Physiol Res* 2001; **50**: 537–546.
38 Uzu T, Sawaguchi M, Maegawa H, Kashiwagi A. Impact of renin-angiotensin system inhibition on microalbuminuria in type 2 diabetes: a *post hoc* analysis of the Shiga Microalbuminuria Reduction Trial (SMART). *Hypertens Res* 2008; **31**: 1171–1176.
39 Liu F, Wei CC, Wu SJ, Chenier I, Zhang SL, Filep JG, Ingelfinger JR, Chan JS. Apocynin attenuates tubular apoptosis and tubulointerstitial fibrosis in transgenic mice independent of hypertension. *Kidney Int* 2009; **75**: 156–166.
40 Burnier M. Telmisartan: a different angiotensin II receptor blocker protecting a different population? *J Int Med Res* 2009; **37**: 1662–1679.
41 Kakuta H, Sudoh K, Sasamata M, Yamagishi S. Telmisartan has the strongest binding affinity to angiotensin II type 1 receptor: comparison with other angiotensin II type 1 receptor blockers. *Int J Clin Pharmacol Res* 2005; **25**: 41–46.
42 Dobrian AD, Schriver SD, Khraibi AA, Prewitt RL. Pioglitazone prevents hypertension and reduces oxidative stress in diet-induced obesity. *Hypertension* 2004; **43**: 48–56.
43 Kiritoshi S, Nishikawa T, Sonoda K, Kukidome D, Senokuchi T, Matsuo T, Matsumura T, Tokunaga H, Brownlee M, Araki E. Reactive oxygen species from mitochondria induce cyclooxygenase-2 gene expression in human mesangial cells: potential role in diabetic nephropathy. *Diabetes* 2003; **52**: 2570–2577.
44 Ditzel J, Schwartz M. Abnormally increased glomerular filtration rate in short-term insulin-treated diabetic subjects. *Diabetes* 1967; **16**: 264–267.
45 Hostetter TH, Troy JL, Brenner BM. Glomerular hemodynamics in experimental diabetes mellitus. *Kidney Int* 1981; **19**: 410–415.

Diabetes, Obesity and Metabolism 2011.

Comparisons of the effects of 12-week administration of miglitol and voglibose on the responses of plasma incretins after a mixed meal in Japanese type 2 diabetic patients

To compare the effects of miglitol [an alpha-glucosidase inhibitor (AGI) absorbed in the intestine] and voglibose (an AGI not absorbed) on plasma glucagon-like peptide-1 (GLP-1) and gastric inhibitory polypeptide (GIP) levels, 26 and 24 Japanese type 2 diabetic patients were randomly assigned to receive miglitol or voglibose, respectively. After 12-week administration of both drugs, during 2-h meal tolerance test, plasma glucose, serum insulin and total GIP were significantly decreased and active GLP-1 was significantly increased. Miglitol group showed a significantly lower total GIP level than voglibose group. Miglitol, but not voglibose, significantly reduced body weight (BW). In all participants, the relative change in BW was positively correlated with that of insulin significantly and of GIP with a weak tendency, but not of GLP-1. In conclusion, both drugs can enhance postprandial GLP-1 responses and reduce GIP responses. The significant BW reduction by miglitol might be attributable to its strong GIP-reducing efficacy.

Keywords: diabetes, incretin, GIP, GLP-1, miglitol, voglibose

Date submitted 16 June 2011; date of first decision 26 July 2011; date of final acceptance 21 October 2011

Introduction

Novel approaches to the treatment of type 2 diabetes (T2D) have focused on strategies for enhancing the action of glucagon-like peptide-1 (GLP-1), such as the use of GLP-1 mimetics and dipeptidyl peptidase-4 (DPP-4) inhibitors. Gastric inhibitory polypeptide (GIP), another incretin, has also been shown to have a physiological role on fat accumulation into adipose tissues [1]. In patients with obesity and insulin resistance, reducing the GIP signal may be a novel therapeutic strategy to prevent and cure T2D.

In studies with healthy controls, administration of alpha-glucosidase inhibitors (AGIs) leads to a reduction in the postprandial GIP responses and a prolonged enhancement of the GLP-1 responses. However, a few studies with a small number of patients with T2D, including our own, have reported controversial effects of AGIs on GLP-1 (no change following acarbose or voglibose administration, [2–4]; increase following miglitol administration [4–6]) and GIP (no change following voglibose administration [4], decrease following acarbose and miglitol administration [2,4–6]) plasma levels after ingestion of a mixed meal. Furthermore, it is unclear whether these effects of AGIs differ based on the type of AGI used and whether they are preserved after long-term administration.

Miglitol is an AGI absorbed in the upper portion of the small intestine, resulting in the diminished efficacy of AGI at the lower portion of the small intestine. Therefore, in the clinical use of miglitol, a sufficient dosage with strong AGI efficacy can be administered with lower incidence of gastro-intestinal adverse events compared with other AGIs not absorbed in the intestine [7].

Therefore, we attempted to compare the effects of 12 week of treatment with miglitol and voglibose (an AGI not absorbed in the intestine) on the responses of plasma incretins after a mixed meal in Japanese patients with T2D.

Patients and Methods

This 12-week, multi-center, open, randomized parallel controlled study included 50 Japanese patients with T2D, who were treated with diet therapy alone or with oral hypoglycaemic agents other than AGIs. All patients were instructed to continue their usual diet and medications through the study.

Before and after the 12-week administration of miglitol or voglibose (50 mg of miglitol or 0.3 mg of voglibose thrice a day immediately before every meal), all patients underwent a 2-h meal tolerance test (MTT) performed in the morning after an overnight fast; the meal consisted of 460 kcal of total caloric load with 56.5 g of carbohydrates, 18 g of protein and 18 g of fat.

During the MTT, blood samples were collected at 0, 30, 60 and 120 min. For determination of the plasma levels of active GLP-1 and total GIP, tubes (Mitsubishi Chemical Medience Co., Tokyo, Japan) containing EDTA-2Na and Diprotin A (a DPP-4 inhibitor) were used. Active GLP-1 and total GIP levels were measured using commercially available ELISA kits (Millipore Corporation, Billerica, MA, USA). Active GLP-1 was

Correspondence to: Takuma Narita, Department of Endocrinology, Diabetes and Geriatric Medicine, Akita University School of Medicine, Hondo 1-1-1, Akita 010-8543 Japan.
E-mail: narita@med.akita-u.ac.jp

measured using plasma prepared with solid phase extraction (Oasis HLB Extraction Plate, Waters Corporation, Milford, MA, USA). The value for haemoglobin A1c (HbA1c) (%) was estimated as a National Glycohemoglobin Standardization Program (NGSP) equivalent value (%) calculated by the formula HbA1c (NGSP) (%) = HbA1c as defined by the Japan Diabetes Society (%) + 0.4%.

As there are no reports focusing on differences in the specific chronic effects of different types of AGIs on circulating incretin levels in humans, we could not predefine an appropriate sample size. Therefore, this study should be considered as exploratory research.

The study protocol was approved by the ethics committee of each participating institute. All participants provided their written informed consent. This study has been registered in the University Hospital Medical Information Network (UMIN) Clinical Trials Registry System as trial ID 000001671.

Results

Clinical characteristics of the 50 patients (26 miglitol and 24 voglibose recipients) are shown in the Table 1. Both drugs significantly decreased HbA1c levels, whereas the fasting plasma glucose (PG), insulin and serum lipid levels were not affected. Only miglitol decreased body weight (BW) and body mass index significantly.

PG, insulin, total GIP and active GLP-1 responses during the MTT (figure 1) at baseline were comparable in both groups. Following the administration of both drugs, PG and insulin levels measured at 30 and 60 min during the MTT were significantly lower than those measured at baseline, except for the insulin levels measured at 30 min in the voglibose group. During the second MTT, PG levels at 30 min were significantly lower in the miglitol group than in the voglibose group. In the miglitol group, PG levels at 120 min during the second MTT were higher than those at 60 min, whereas in the voglibose group, PG levels at 120 min were lower than those at 60 min.

Postprandial total GIP levels during the second MTT were significantly lower than baseline in both groups, with a lower overall level observed in the miglitol group compared with the voglibose group (Table 1 and figure 1C). The active GLP-1 area under the curve (AUC) was higher compared with baseline after the administration of both drugs (Table 1). Active GLP-1 at 60 min was higher after administration of both drugs, whereas

Table 1. Clinical characteristics of participants and relative changes from baseline values of the integrated responses of plasma glucose (PG), serum insulin, total gastric inhibitory polypeptide (GIP) and active glucagon-like peptide-1 (GLP-1) during a 2-h meal tolerance test.

	Miglitol		Voglibose	
	Baseline	12 weeks	Baseline	12 weeks
Male/Female, n	14/12		18/6	
Age (years)	58.5 ± 9.9		59.5 ± 11.6	
Duration (years)	9.9 ± 6.7		9.1 ± 6.6	
Use of OADs, n (%)	21 (80.8)		20 (83.3)	
Use of SU, n (%)	17 (65.4)		15 (62.5)	
Use of MET, n (%)	16 (61.5)		17 (70.8)	
Use of TZD, n (%)	9 (34.6)		11 (45.8)	
Body weight (kg)	64.5 ± 14.0	63.6 ± 14.0**	69.4 ± 18.7	69.3 ± 18.6
BMI (kg/m^2)	25.1 ± 5.2	24.7 ± 5.1*	25.6 ± 5.0	25.6 ± 4.9
FPG (mmol/l)	8.4 ± 1.3	8.3 ± 1.3	8.8 ± 2.7	8.2 ± 1.8
Fasting insulin (pmol/l)	30.0 ± 22.6	27.5 ± 19.7	29.9 ± 31.1	31.9 ± 40.5
TC (mmol/l)	5.40 ± 0.61	5.60 ± 0.70	5.17 ± 0.73	5.40 ± 0.98
TG (mmol/l)	1.48 ± 0.71	1.55 ± 0.98	1.39 ± 0.46	1.49 ± 0.99
HDLc (mmol/l)	1.51 ± 0.42	1.55 ± 0.53	1.52 ± 0.40	1.48 ± 0.35
HbA1c (%)	7.51 ± 0.47	7.35 ± 0.61*	7.49 ± 0.70	7.13 ± 0.71*
Δ from baseline (%)		−0.16 ± 0.39		−0.36 ± 0.39
PG AUC (h.mmol/l)	23.9 ± 0.81	19.5 ± 0.57***	23.4 ± 0.69	20.2 ± 0.76***
Relative changes (%)		−17.0 ± 2.5$		−12.8 ± 2.0
Insulin AUC (h.pmol/l)	210.5 ± 24.5	149.5 ± 20.0***	214.5 ± 45.0	182.0 ± 42.0**
Relative changes (%)		−24.9 ± 5.6		−10.6 ± 5.8
GIP AUC (h.pg/ml)	752.4 ± 54.2	385.5 ± 31.0***,†	813.5 ± 71.6	489.6 ± 33.9***
Relative changes (%)		−47.9 ± 2.3‡		−35.4 ± 4.6
GLP-1 AUC (h.pmol/l)	8.3 ± 0.84	11.4 ± 0.92***	8.5 ± 0.74	10.1 ± 0.98*
Relative changes (%)		+52.0 ± 10.3‡		+33.0 ± 14.2

Data are expressed as mean ± SD unless otherwise indicated. BMI, body mass index; FPG, fasting plasma glucose; TC, total cholesterol; TG, triglyceride; HDLc, high-density lipoprotein cholesterol; OADs, oral anti diabetic agents; SU, sulfonylurea; MET, metformin; TZD, thiazolidinedione; Δ from baseline (%), changes from baseline values; Relative changes (%), relative changes (%) of the respective parameters at 12 weeks from baseline values; AUC, area under the curve during the 2-h meal tolerance test.

*$p < 0.05$, **$p < 0.01$ and ***$p < 0.001$ vs. baseline values revealed by the Wilcoxon signed-ranks test, respectively.

†$p < 0.05$ vs. voglibose treatment revealed by the Mann–Whitney *U*-test.

‡$p < 0.01$ and $ $p < 0.001$ vs. voglibose treatment revealed by the analysis of covariance (ANCOVA) model with the respective baseline values as covariates.

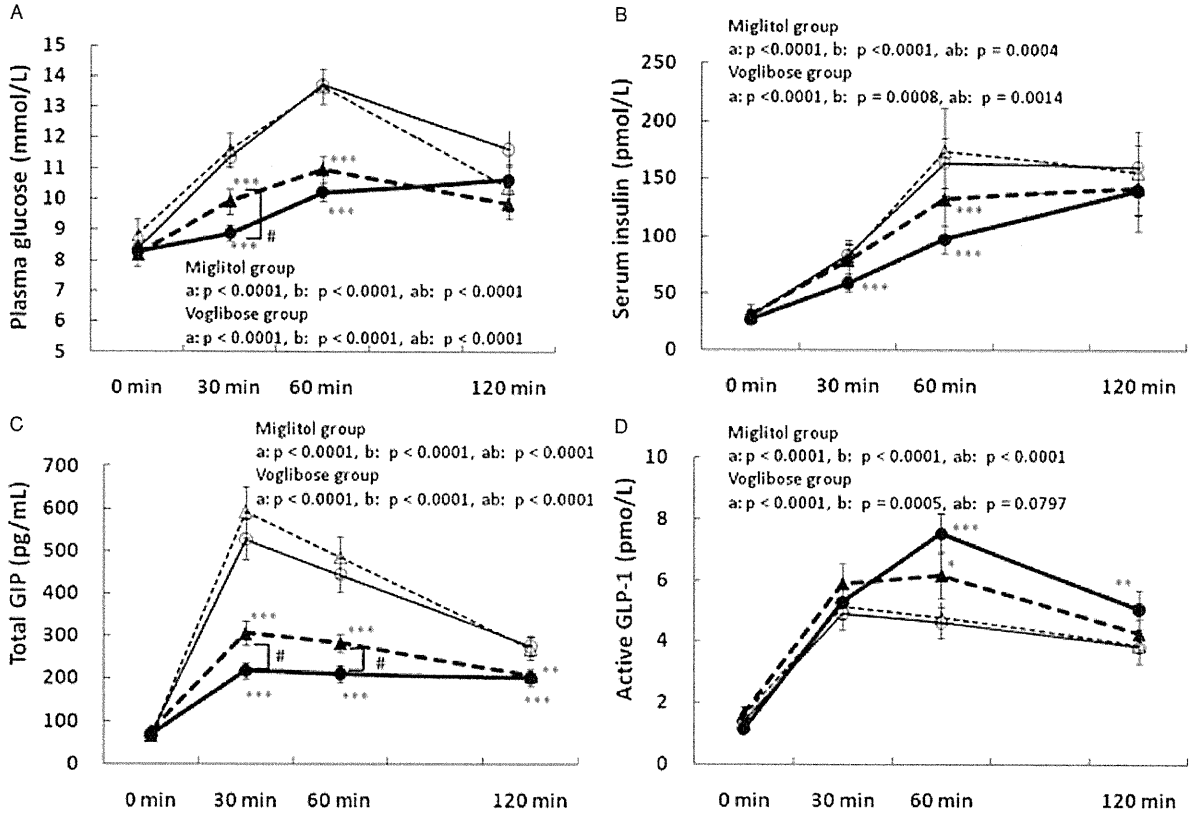

Figure 1. The effects of 12-week administration of miglitol and voglibose on changes in plasma glucose (A), serum insulin (B), plasma total gastric inhibitory polypeptide (GIP) (C) and plasma active glucagon-like peptide-1 (GLP-1) (D) in response to ingestion of a mixed meal. Values are expressed as mean ± SE. Open circle, before miglitol; closed circle, after miglitol; open triangle, before voglibose; closed triangle, after voglibose. p-Values represent differences according to treatment (a), over time course (b), and the interaction of treatment and time course (ab) as calculated by repeated-measures analysis of variance. *, ** and ***, significant differences ($p < 0.05$, $p < 0.01$ and $p < 0.001$, respectively) at individual time points by the Wilcoxon-signed ranks test. #, $p < 0.05$ between miglitol and voglibose by the Mann–Whitney *U*-test.

active GLP-1 at 120 min was higher only after administration of miglitol, compared with baseline (Figure 1D).

An analysis of covariance (ANCOVA) with the respective baseline values as covariates revealed that the relative changes (%) from baseline in the PG AUC, total GIP AUC and active GLP-1 AUC at 12 weeks were significantly different between miglitol and voglibose (Table 1).

Pearson's correlation analyses were performed to assess the relationships between the relative changes from baseline (%) in the AUCs of plasma incretins and those in the PG AUC, the insulin AUC and the ratio of incremental AUC from 0 min during the MTT of insulin to that of PG (iAUC-insulin/iAUC-PG). Among all participants, the relative change in the total GIP AUC was correlated with that in the insulin AUC ($r = +0.3702$, $p < 0.01$), whereas the relative change in the active GLP-1 AUC was correlated with that in the iAUC-insulin/iAUC-PG ($r = +0.2990$, $p < 0.05$).

The relative change in BW was positively and significantly correlated with the change in the insulin AUC ($r = +0.320$, $p < 0.05$) and also showed a weak correlation with the change in the GIP AUC ($r = +0.262$, $p = 0.066$) among all participants. The relative change in BW was positively correlated with the HbA1c change from baseline in the miglitol group ($r = +0.4121$, $p < 0.05$) but not in the voglibose group ($r = -0.3181$, $p = 0.1298$).

Discussion

To our knowledge, this study is the first to show that relatively long-term (12-week) administration of both miglitol and voglibose significantly increases the responses of active GLP-1 and decreases the responses of total GIP after ingestion of a mixed meal in patients with T2D.

In this study, miglitol showed a lower level of postprandial total GIP and a higher level of active GLP-1 in ANCOVA comparisons with voglibose. The results may have affected the difference in postprandial PG levels between miglitol and voglibose. One of the limitations of this study is the lack of a placebo arm. Therefore, it is necessary to wait for future, more statistically robust investigations before concluding that miglitol has a stronger effect on circulating incretin levels than voglibose.

The relative change in the total GIP AUC was correlated with that in the insulin AUC, with both parameters being reduced in this study, suggesting the effective suppression of carbohydrates absorption in the upper intestine by the two drugs. However,

direct causality between the two hormones is unclear as the insulinotropic effect of GIP is almost abolished in patients with T2D [8]. In contrast, the relative change in the active GLP-1 AUC correlated with that in the iAUC-insulin/iAUC-PG, suggesting improvement of beta cell function through the increased active GLP-1 AUC.

During the second MTT, PG at 30 min during MTT was significantly lower in the miglitol group than in the voglibose group, and the peak PG was delayed from 60 to 120 min after miglitol administration but not after voglibose administration (figure 1), indicating that miglitol, an AGI absorbed in the intestine, induces a relatively lower degree of carbohydrate absorption in the GIP-secreting upper portion of the intestine, and a higher degree of carbohydrate absorption in the GLP-1-secreting lower portion of the intestine than voglibose, which is not absorbed in the intestine. This may also explain the present result, namely the significantly lower level of total GIP and the relatively higher level of active GLP-1 observed in the miglitol group compared with the voglibose group.

In previous studies among patients with T2D, miglitol and acarbose suppressed postprandial GIP responses regardless of AGI dosage or duration of administration [2,4–6]. In contrast, a single and low-dose (0.3, 0.5 and 1.0 mg) administration of voglibose did not suppress either of postprandial PG, insulin or GIP responses [4,9], whereas a prolonged administration of low dose voglibose did suppress these responses, both in healthy subjects (0.5 and 1.0 mg) [9] and in our patients with T2D (0.3 mg), indicating the necessity of a prolonged administration of low-dose voglibose for significant efficacy.

No enhancement of GLP-1 response by acarbose has previously been found among obese patients with poorly controlled T2D (HbA1c, 7.8% [2]; 8.22% [3]), but such an enhancement was revealed among patients with T2D who had relatively good glycaemic control (HbA1c, 6.7–7.0% [4–6]) and who were administered miglitol. Therefore, the positive enhancement of the effects of GLP-1 responses induced by miglitol and voglibose in this study may be partially attributed to the relatively good glycaemic control among our patients (HbA1c, approximately 7.5%). Furthermore, obesity attenuates the GLP-1 response to carbohydrates [10], and none of our patients was severely obese; this may partially explain our present result of the significant enhancement of the postprandial GLP-1 response after administration of both drugs.

The mechanism behind the increase in postprandial active GLP-1 levels after the administration of both drugs is probably attributable to enhanced secretion of GLP-1 and/or inhibition of DPP-4 activity. Because postprandial total GLP-1 levels (measured with antisera against carboxy-terminus of GLP-1) increased after the administration of AGIs in previous studies, including our own [6,11], suggesting increased GLP-1 secretion, we did not measure total GLP-1 levels but measured only active GLP-1 levels, which directly induce insulin secretion and other effects of GLP-1. Interestingly, a recent study in mice reported that voglibose administration decreased DPP-4 activity through a reduction in the DPP-4 protein level despite increases in the gut GLP-1 content and both total and active plasma GLP-1 levels [12]. Accordingly, simultaneous measurements of both GLP-1 and GIP in its active and total forms, as well as DPP-4 activity and its protein levels before and after AGIs usage is warranted in future studies.

We used the highest dose of voglibose (0.3 mg thrice a day) but not the highest dose of miglitol (50 mg and not 75 mg thrice a day) permitted in Japan because a previous crossover study reported that only a single 50 mg dose of miglitol can modulate PG, active GLP-1 and total GIP levels but not a single 0.3 mg dose of voglibose [4]. It remains to be elucidated whether the highest dose of miglitol (75 mg thrice a day) would have a stronger effect on modulating postprandial circulating incretin levels than the dose used in this study.

It is also unclear whether miglitol or voglibose themselves have the potential to increase active GLP-1 levels. In one study in mice [12], DPP-4 activity was not influenced by the addition of voglibose to the plasma. Furthermore, in a study of healthy human subjects [11], plasma GLP-1 levels did not change during ingestion of a carbohydrate-free meal with acarbose. These results suggest that AGIs enhance circulating GLP-1 levels only after their administration with carbohydrates.

In this study, the reduction in BW was positively correlated with that in GIP with a weak tendency and there was a positive correlation between the reductions of HbA1c and BW only in the miglitol group. The postprandial GIP response was significantly lowered after miglitol administration than after voglibose administration. In animal experiments of excess nutrient intake, reducing the GIP signal in a physiological level results in improvement of obesity, insulin resistance and glucose tolerance accompanied with prevention of fat accumulation into adipocytes and high energy expenditure, [1]. Taken together, these findings suggest that sufficient suppression of the GIP signal by miglitol is a preferable therapeutic option for obese patients with T2D.

T. Narita[1], H. Yokoyama[2], R. Yamashita[2], T. Sato[1], M. Hosoba[1], T. Morii[1], H. Fujita[1], K. Tsukiyama[3] & Y. Yamada[1]

[1]Department of Endocrinology, Diabetes and Geriatric Medicine, Akita University Graduate School of Medicine, Akita, Japan
[2]Jiyugaoka Medical Clinic, Internal Medicine, Obihiro, Japan
[3]Department of Metabolism and Clinical Nutrition, Akita University School of Medicine, Akita, Japan

Acknowledgements

The study was supported in part by Grants-in-Aid from the Japanese Ministry of Education, Culture, Sports, Science and Technology and from the Japanese Ministry of Health, Labour and Welfare. Parts of this study were presented as a poster at the 46th annual meeting of the European Association for the Study of Diabetes, Stockholm, Sweden, 20–24 September 2010.

Conflict of Interest

The authors have no conflict of interest to declare.

T. N. and H. Y. contributed to design, conduct/data collection, analysis and writing of the manuscript. R. Y.